Computers and Mathematics with Applications 77 (2019) 2833–2853

Contents lists available at ScienceDirect

Computers and Mathematics with Applications

journal homepage: www.elsevier.com/locate/camwa

A posteriori error estimates of finite element method for the time-dependent Darcy problem in an axisymmetric domain

Ajmia Younes Orfi [a], Driss Yakoubi [b,*]

[a] University of Tunis El Manar, Faculty of Sciences, 2060 Tunis, Tunisia
[b] GIREF, Département de Mathématiques et Statistiques, Université Laval, Québec, Canada

ARTICLE INFO

Article history:
Received 6 October 2016
Received in revised form 20 October 2018
Accepted 18 January 2019
Available online 10 February 2019

Keywords:
Darcy's equations
Axisymmetric domain
Fourier truncation
Finite element discretization
A posteriori analysis

ABSTRACT

We consider the time dependent Darcy problem in a three-dimensional axisymmetric domain and, by writing the Fourier expansion of its solution with respect to the angular variable, we observe that each Fourier coefficient satisfies a system of equations on the meridian domain. We propose a discretization of these equations in the case of general solution. This discretization relies on a backward Euler's scheme for the time variable and finite elements for the space variables. We prove a posteriori error estimates that allow for an efficient adaptivity strategy both for the time steps and the meshes. Computations for an example with a known solution are presented which support the a posteriori error estimate.

1. Introduction

Let $\breve{\Omega}$ be a bounded axisymmetric domain in $\mathbb{R}^3$. The boundary $\breve{\Gamma}$ of this domain is divided into two parts $\breve{\Gamma}_p$ and $\breve{\Gamma}_u$. We are interested in the following model, suggested by Rajagobal [1],

$$\begin{cases} \partial_t \breve{\boldsymbol{u}} + \alpha \breve{\boldsymbol{u}} + \mathbf{grad} \breve{p} = \breve{\boldsymbol{f}} & \text{in } \breve{\Omega} \times]0, T[, \\ \mathrm{div} \breve{\boldsymbol{u}} = 0 & \text{in } \breve{\Omega} \times]0, T[, \\ \breve{p} = \breve{p}_b & \text{on } \breve{\Gamma}_p \times]0, T[, \\ \breve{\boldsymbol{u}} \cdot \breve{\boldsymbol{n}} = \breve{g} & \text{on } \breve{\Gamma}_u \times]0, T[, \\ \breve{\boldsymbol{u}} = \breve{\boldsymbol{u}}_0 & \text{in } \breve{\Omega} \text{ at time } t = 0. \end{cases} \tag{1.1}$$

where the unknowns are the velocity $\breve{\boldsymbol{u}}$ and the pressure $\breve{p}$ of the fluid. The data are the quantities $\breve{\boldsymbol{f}}$, $\breve{g}$, the pressure on the boundary $\breve{p}_b$ and the initial value of the velocity $\breve{\boldsymbol{u}}_0$. The parameter α is a positive constant representing the drag coefficient. This model can represent the time-dependent flow of an incompressible fluid such as water in a rigid porous material. If the problem is set in a domain which is symmetric by rotation around an axis, it is proved in [2] that, when using the Fourier expansion with respect to the angular variable, a three-dimensional problem is equivalent to a system of two-dimensional problems on the so-called meridian domain noted Ω and defined below, see (2.1). Each obtained problem being satisfied by a Fourier coefficient of the solution. We recall that in [3], the present problem has already been considered in the case of an axisymmetric solution, in the other words, for the Fourier coefficient of order $k = 0$. In the present paper, we will extend the analysis in the case of a general solution, i.e. for the Fourier coefficient of order k, $k \in \mathbb{Z}$. We will deal with the instationary Darcy system in three-dimensional axisymmetric geometries and propose its discretization in order to

* Corresponding author.
E-mail addresses: ayounesorfi@yahoo.com (A.Y. Orfi), yakoubi@giref.ulaval.ca (D. Yakoubi).

https://doi.org/10.1016/j.camwa.2019.01.016
0898-1221/

approximate this general solution. We also recall that the problem considered in [4] which is similar to the present model is restricted to a boundary condition for the pressure and when the domain is a general two- or three-dimensional with a Lipschitz-continuous boundary. So, in the present study, we shall handle the mixed boundary conditions which are more realistic from a physical point of view. indeed, most often, only one of these conditions can be measured on part of the boundary.

Up to our knowledge, the first work that has been done on the a priori analysis of the present problem is due to Orfi et al. [5]. The aim of this paper is to perform the a posteriori analysis of the discretization.

Several work has been done concerning the a posteriori analysis of parabolic type problems. In [6–8] the idea consists in establishing a full time and space variational formulation of the continuous problem and using a discontinuous Galerkin method for the discretization with respect to all variables.

In this work, following the approach of [9], which consists in introducing different types of error indicators: one for the time discretization and another for the space discretization, we perform the a posteriori error analysis and prove optimal estimates of the error according to the standard criteria see [10] for a review of the main results in a posteriori analysis. Therefore the error indicators that we propose seem appropriate tools for performing time and space adaptivity in an efficient way. Our analysis is performed when the boundary conditions and the external forces are assumed in general case. Therefore, axisymmetric problems without any assumption on the data can be transformed into problems which are invariant by rotation see [11, Chap I, prop 1.2.8]. A natural way for reducing axisymmetric problems on $\breve{\Omega}$ to a family of problems on the meridian domain Ω, which we will make precise later, relies on the use of Fourier expansions with respect to the angular variable θ.

The paper is organized as follows: In Section 2, we start by writing the variational formulation of problem (1.1) in the case of an axisymmetric domain, its well-posedness and also the error arising from Fourier truncation. Next, we describe the discrete problem in the meridian domain Ω in Section 3. The error due to Fourier truncation which was appropriately evaluated in [5] is also devoted in this section. We introduce two families of error indicators in Section 4: one corresponds to the time discretization and others associate to the finite element space. We then perform the a posteriori analysis of the discrete problem in several steps. Section 5 is devoted to the description of the adaptivity strategy we use . In Section 6, we present some numerical experiments. Finally, Conclusion 7 concerns the main concluding remarks.

2. The two-dimensional problems

Let (x, y, z) be a set of Cartesian coordinates in $\mathbb{R}^3$ such that $\breve{\Omega}$ is invariant by rotation around the axis $x = y = 0$. We introduce the system of cylindrical coordinates (r, θ, z), with $r \geq 0$ and $-\pi \leq \theta < \pi$, defined by $x = r\cos\theta$ and $y = r\sin\theta$. If Γ_0 denotes the intersection between $\breve{\Omega}$ and axis $r = 0$, then there exists an open bounded domain Ω in $\mathbb{R}_+ \times \mathbb{R}$ such that

$$\breve{\Omega} = \{(r, \theta, z); (r, z) \in \Omega \cup \Gamma_0 \quad \text{and} \; -\pi < \theta \leq \pi\}. \tag{2.1}$$

The set Ω is called meridian domain. For simplicity, we assume that Γ_0 is the union of a finite number of segments with positive measure. The two-dimensional axisymmetric boundary $\breve{\Gamma}$ of the physical domain $\breve{\Omega}$ is a Lipschitz-continuous boundary and is divided into two parts $\breve{\Gamma}_p$ and $\breve{\Gamma}_u$, also with Lipschitz continuous boundaries. The part of the boundary $\breve{\Gamma}_p$ has a positive surface measure. $\breve{\Gamma}_u = \breve{\Gamma} \setminus \overline{\breve{\Gamma}}_p$ is the union of a finite number of surface elements. Setting $\Gamma = \partial\Omega \setminus \Gamma_0$ and rotating Γ around the axis $r = 0$ gives back $\breve{\Gamma}$, and Γ_0 is a kind of artificial boundary. We also introduce the two parts Γ_p and $\Gamma_u = \Gamma \setminus \overline{\Gamma}_p$ of the boundary Γ. The unit outward normal vector $\breve{\boldsymbol{n}}$ on $\breve{\Gamma}$ is obtained by rotating the unit outward vector $\boldsymbol{n}$ on Γ.

Each solution of the Darcy equations admits a Fourier expansion with respect to the angular variable θ.

2.1. Fourier expansion

For any function $\breve{v}$ defined on $\breve{\Omega}$, we associate the Fourier coefficients of the corresponding function v on Ω, defined for any k in $\mathbb{Z}$ by

$$v^k(r, z) = \frac{1}{\sqrt{2\pi}} \int_{-\pi}^{\pi} v(r, \theta, z)\, e^{-ik\theta} d\theta, \quad v(r, \theta, z) = \frac{1}{\sqrt{2\pi}} \sum_{k\in\mathbb{Z}} v^k(r, z) e^{ik\theta}.$$

We also introduce the k-dependent operators $\textbf{grad}_k p$ and $\text{div}_k \boldsymbol{v}$ defined respectively for scalar functions p and on vector fields $\boldsymbol{v}$ by

$$\textbf{grad}_k p = (\partial_r p,\ \frac{ik}{r} p,\ \partial_z p) \qquad \text{and} \qquad \text{div}_k \boldsymbol{v} = \partial_r v_r + \frac{1}{r} v_r + \frac{ik}{r} v_\theta + \partial_z v_z.$$

It is checked in [11, IX.1] that $(\breve{\boldsymbol{u}}, \breve{p})$ is solution to problem (1.1) if and only if the pairs $(\boldsymbol{u}_k, p_k)$, $k \in \mathbb{Z}$, are solutions to the system of two-dimensional problems

$$\left\{\begin{array}{rcll} \partial_t \boldsymbol{u}^k + \alpha \boldsymbol{u}^k + \textbf{grad}_k p^k &=& \boldsymbol{f}^k & \text{in} \quad \Omega \times]0, T[, \\ \text{div}_k \boldsymbol{u}^k &=& 0 & \text{in} \quad \Omega \times]0, T[, \\ p^k &=& p_b^k & \text{on} \quad \Gamma_p \times]0, T[, \\ \boldsymbol{u}^k \cdot \boldsymbol{n} &=& g^k & \text{on} \quad \Gamma_u \times]0, T[, \\ \boldsymbol{u}^k &=& \boldsymbol{u}_0^k & \text{in} \quad \Omega \text{ at } t = 0. \end{array}\right. \tag{2.2}$$

We now describe the weighted Sobolev spaces which are needed for the variational formulations of these problems, next we write these formulations, we recall their well-posedness and the error arising from Fourier truncation.

2.2. The weighted Sobolev spaces

Consequently, this reduction to 2-D problems requires the numerical analysis to be studied in suitably weighted Hilbert spaces, which deal with complex-valued functions due to Fourier expansions, see for instance [2, Sec. II.2]:

$$\begin{aligned} L^2_{\pm 1}(\Omega) &= \left\{ v : \Omega \to \mathbb{C} \text{ measurable}; \ \int_\Omega |v(r,z)|^2 \, r^{\pm 1} \, dr\, dz < +\infty \right\}, \\ H^1_1(\Omega) &= \left\{ v \in L^2_1(\Omega); \ \partial_r v \in L^2_1(\Omega) \text{ and } \partial_z v \in L^2_1(\Omega) \right\}, \\ H^1_{1\diamond}(\Omega) &= \left\{ q \in H^1_1(\Omega); \ q = 0 \text{ on } \Gamma_p \right\}, \\ \text{and} \quad & V^1_1(\Omega) = H^1_1(\Omega) \cap L^2_{-1}(\Omega), \qquad V^1_{1\diamond}(\Omega) = V^1_1(\Omega) \cap H^1_{1\diamond}(\Omega). \end{aligned}$$

All these spaces are provided with the norms which result from their definitions.

For any $k \in \mathbb{Z}$, we denote by $H^1_{(k)}(\Omega)$ the following spaces

$$H^1_{(k)}(\Omega) = \begin{cases} H^1_1(\Omega) & \text{if } k = 0, \\ V^1_1(\Omega) & \text{if } |k| \geq 1, \end{cases}$$

equipped with norms and seminorms:

$$\|v\|_{H^1_{(k)}(\Omega)} = \left(\|v\|^2_{H^1_1(\Omega)} + |k|^2 \, \|v\|^2_{L^2_{-1}(\Omega)} \right)^{\frac{1}{2}} \text{ and } |v|_{H^1_{(k)}(\Omega)} = \left(|v|^2_{H^1_1(\Omega)} + |k|^2 \, \|v\|^2_{L^2_{-1}(\Omega)} \right)^{\frac{1}{2}}.$$

We also define the subspaces $H^1_{(k)\diamond}(\Omega) = H^1_{(k)}(\Omega) \cap H^1_{1\diamond}(\Omega)$. Note that the equivalence of the norm $\|\cdot\|_{H^1_{(k)}(\Omega)}$ and seminorm $|\cdot|_{H^1_{(k)}(\Omega)}$ on $H^1_{(k)\diamond}(\Omega)$, which is obvious for $k \neq 0$, also holds for $k = 0$ (see [2, Thm. II.3.1]).

Let us introduce the space $H^{\frac{1}{2}}_{(k)}(\Gamma_p)$ of traces of functions in $H^1_{(k)}(\Omega)$ on Γ_p. The trace on Γ_u is defined in a nearly standard way see [11, Sec. 2]. We use the whole scale of Sobolev spaces $H^s_1(\Gamma_u)$, $s \geq 0$, as defined in [2, Chap. II] from

$$L^2_1(\Gamma_u) = \left\{ g : \Gamma_u \to \mathbb{R} \text{ measurable}; \ \int_{\Gamma_u} g^2(\tau) r(\tau) \, d\tau < +\infty \right\},$$

where $r(\tau)$ denotes the distance of the point with tangential coordinate τ to the axis $r = 0$. The trace operator: $v \longmapsto v_{|\Gamma_u}$ is continuous and surjective from $H^{s+1}_1(\Omega)$ onto $H^{s+\frac{1}{2}}_1(\Gamma_u)$, $s \geq 0$, and in particular from $H^1_1(\Omega)$ onto $H^{\frac{1}{2}}_1(\Gamma_u)$ and also from $V^1_1(\Omega)$ onto the same space $H^{\frac{1}{2}}_1(\Gamma_u)$, see [2, Chap.II].

We introduce the spaces $H^{m,s}(\breve{\Omega})$, (see [2, Sec. II.4.b])

$$H^{m,s}(\breve{\Omega}) = \left\{ \breve{v} \in H^m(\breve{\Omega}); \quad \partial^\ell_\theta \breve{v} \in H^m(\breve{\Omega}), \ 1 \leq \ell \leq s \right\}$$

and evident extension of spaces defined on each part of $\partial\breve{\Omega}$, where $m \in \mathbb{R}$ and $s \geq 0$. Note that $H^{m,0}(\breve{\Omega})$ coincides with $H^m(\breve{\Omega})$.

From [2, Thm. II.3.1], we obtain the following characterization of $H^{m,s}(\breve{\Omega})$ by Fourier coefficients.

Lemma 2.1. *For any nonnegative real number s and any integer m, the norm* $\left(\sum_{k \in \mathbb{Z}} (1 + |k|^2)^s \left\| v^k \right\|^2_{H^m_{(k)}(\Omega)} \right)^{\frac{1}{2}}$ *is equivalent, on* $H^{m,s}(\breve{\Omega})$*, to the norm induced by the definition of this space.*

Where $H^0_{(k)}(\Omega) = L^2_1(\Omega)$, $|k| \geq 0$ and $H^1_{(k)}(\Omega) = V^1_1(\Omega)$, $|k| \geq 1$.

Remark 2.2. When m is a negative integer, we denote by $H^m_{(k)\diamond}(\Omega)$ the dual space of $H^{-m}_{(k)}(\Omega) \cap H^{-m}_{1\diamond}(\Omega)$ and provided with the dual norm.

For convenience, throughout this paper, we will use the notation $x \lesssim y$ to denote that $x \leq cy$, where c is a positive constant.

2.3. Weak formulation

We assume that the datum $\boldsymbol{u}^k_0$ belongs to $L^2_1(\Omega)^3$ and that the data $(\boldsymbol{f}^k, p^k_b, g^k)$ belong to $L^2\big(0,T; L^2_1(\Omega)^3\big) \times L^2\big(0,T; H^{\frac{1}{2}}_{(k)}(\Gamma_p)\big) \times L^2\big(0,T; L^2_1(\Gamma_u)\big)$. Then, the Fourier coefficients $\big((\boldsymbol{u}^k, p^k)\big)_{k \in \mathbb{Z}}$ of a solution of problem (2.2) are a solution of:

Find $(\boldsymbol{u}^k, p^k)$ in $H^1\big(0,T;L^2_1(\Omega)^3\big) \times L^2\big(0,T;H^1_{(k)}(\Omega)\big)$ such that

$$\boldsymbol{u}^k(\cdot,0) = \boldsymbol{u}^k_0 \quad \text{in} \quad \Omega, \tag{2.3}$$

for a.e. $t,\ 0 \le t \le T$,

$$p^k(\cdot,t) = p^k_b \quad \text{on} \quad \Gamma_p, \tag{2.4}$$

$$\begin{aligned} &\forall \boldsymbol{v} \in L^2_1(\Omega)^3, \qquad a_1(\partial_t \boldsymbol{u}^k, \boldsymbol{v}) + \alpha\, a_1(\boldsymbol{u}^k, \boldsymbol{v}) + b^k_1(\boldsymbol{v}, p^k) = (\boldsymbol{f}^k, \overline{\boldsymbol{v}})_1, \\ &\forall q \in H^1_{(k)\diamond}(\Omega), \qquad \overline{b^k_1}(\boldsymbol{u}^k, q) = \int_{\Gamma_u} g^k(\tau)\, q(\tau)\, r(\tau)\, d\tau, \end{aligned} \tag{2.5}$$

where the sesquilinear forms $a_1(\cdot,\cdot)$ and $b^k_1(\cdot,\cdot)$ are defined by:

$$a_1(\boldsymbol{u}, \boldsymbol{v}) = (\boldsymbol{u}, \overline{\boldsymbol{v}})_1 = \int_\Omega \boldsymbol{u}(r,z)\cdot \overline{\boldsymbol{v}}(r,z)\, r\, dr\, dz, \ \text{ and}$$

$$b^k_1(\boldsymbol{v}, p) = (\overline{\boldsymbol{v}}, \operatorname{grad}_k p)_1 = \int_\Omega \overline{\boldsymbol{v}}(r,z)\cdot \operatorname{grad}_k p(r,z)\, r\, dr\, dz.$$

Then, the system consisting of all problems (2.3)–(2.5) has a solution $(\boldsymbol{u}^k, p^k)_{k\in\mathbb{Z}}$ in the product space $\Pi_{k\in\mathbb{Z}} H^1\big(0,T;L^2_1(\Omega)^3\big) \times L^2\big(0,T;H^1_{(k)}(\Omega)\big)$.

These forms are obviously continuous on $L^2_1(\Omega)^3 \times L^2_1(\Omega)^3$ and $L^2_1(\Omega)^3 \times H^1_{(k)}(\Omega)$. Note that $\overline{b^k_1}(\boldsymbol{v}, p) = b^{-k}_1(\overline{\boldsymbol{v}}, \overline{p})$ holds and that the kernel

$$\mathbb{V}_k(\Omega) = \Big\{ \boldsymbol{v} \in L^2_1(\Omega)^3;\ \forall p \in H^1_{(k)\diamond}(\Omega),\ b^k_1(\boldsymbol{v}, p) = 0 \Big\} \quad \text{is characterized by}$$

$$\mathbb{V}_k(\Omega) = \Big\{ \boldsymbol{v} \in L^2_1(\Omega)^3;\ \operatorname{div}_k \boldsymbol{v} = 0 \text{ and } \boldsymbol{v}\cdot\boldsymbol{n} = 0 \text{ on } \Gamma_u \Big\}. \tag{2.6}$$

As standard for saddle-point problems ([12, Chap. I, Thm. 4.1]), the well-posedness of problem (2.3)–(2.5) relies on the ellipticity of $a_1(\cdot,\cdot)$ and on an inf–sup condition of Babuška and Brezzi type on the form $b^k_1(\cdot,\cdot)$:

$$q \in H^1_{(k)\diamond}(\Omega), \ \sup_{\boldsymbol{v}\in L^2_1(\Omega)^3} \frac{b^k_1(\boldsymbol{v}, q)}{\|\boldsymbol{v}\|_{L^2_1(\Omega)^3}} \ge \beta\, |q|_{H^1_{(k)}(\Omega)}, \tag{2.7}$$

$$\forall \boldsymbol{u} \in L^2_1(\Omega)^3, \qquad a_1(\boldsymbol{u}, \boldsymbol{u}) \ge \alpha^1\, \|\boldsymbol{u}\|^2_{L^2_1(\Omega)^3}. \tag{2.8}$$

We refer to [3, Lem. 3] and [4, Thm. 2.4], for the detailed proof of the next Theorem.

Theorem 2.3. *For any data* $(\boldsymbol{f}^k, p^k_b, g^k) \in L^2(0,T;L^2_1(\Omega)^3) \times L^2(0,T;H^{\frac12}_{(k)}(\Gamma_p)) \times L^2(0,T;L^2_1(\Gamma_u))$ *and* $\boldsymbol{u}^k_0 \in L^2_1(\Omega)^3$, *the unique solution* $\big(\boldsymbol{u}^k, p^k\big) \in H^1(0,T;L^2_1(\Omega)^3) \times L^2(0,T;H^1_{(k)}(\Omega))$ *of problem* (2.3)–(2.5) *satisfies the a priori estimate*

$$\begin{aligned} &\|\boldsymbol{u}^k\|_{H^1(0,T;L^2_1(\Omega)^3)} + \|p^k\|_{L^2(0,T;H^1_{(k)}(\Omega))} \lesssim \|\boldsymbol{u}^k_0\|_{L^2_1(\Omega)^3} + \|\boldsymbol{f}^k\|_{L^2(0,T;L^2_1(\Omega)^3)} \\ &+ \|p^k_b\|_{L^2(0,t;H^{\frac12}_{(k)}(\Gamma_p))} + \|g^k\|_{H^1(0,t;L^2_1(\Gamma_u))}. \end{aligned} \tag{2.9}$$

Definition 2.4. With each $\big(\boldsymbol{f}^k, p^k_b, g^k\big)$ in $L^2(0,T;L^2_1(\Omega)^3) \times L^2(0,T;H^{\frac12}_{(k)}(\Gamma_p)) \times L^2(0,T;L^2_1(\Gamma_u))$ and $\boldsymbol{u}^k_0 \in L^2_1(\Omega)^3$, we associate the unique solution $(\boldsymbol{u}^k, p^k)$ of problem (2.3)–(2.5), and we define the three-dimensional functions $\breve{\boldsymbol{u}}$ and $\breve{p}$ by

$$\breve{\boldsymbol{u}}(r,\theta,z) = \frac{1}{\sqrt{2\pi}} \sum_{k\in\mathbb{Z}} \boldsymbol{u}^k(r,z) e^{ik\theta}, \qquad \breve{p}(r,\theta,z) = \frac{1}{\sqrt{2\pi}} \sum_{k\in\mathbb{Z}} p^k(r,z) e^{ik\theta}.$$

It is now readily checked that the corresponding pair $(\breve{\boldsymbol{u}}, \breve{p})$ is the only solution of problem (1.1), so that the Darcy problem is fully equivalent to the problem (2.3)–(2.5), $k \in \mathbb{Z}$.

In the case of axisymmetric data $\breve{\boldsymbol{f}}$, $\breve{p}_b$ and $\breve{g}$, i.e. f_r, f_θ, f_z, p_b and g are independent of θ, all Fourier coefficients of $\big(\breve{\boldsymbol{u}}, \breve{p}\big)$ vanish but those of order zero. We refer to [3] for a slightly different formulation of the problem in this case.

In the case of general data $\breve{\boldsymbol{f}}$, $\breve{p}_b$ and $\breve{g}$, the idea is to solve only a finite number of two-dimensional discrete problems. So, we fix nonnegative integer $\mathcal{K}$, and we introduce the pair $(\breve{\boldsymbol{u}}_{\mathcal{K}}, \breve{p}_{\mathcal{K}})$ which is obtained from $(\breve{\boldsymbol{u}}, \breve{p})$ by Fourier truncation:

$$\breve{\boldsymbol{u}}_{\mathcal{K}}(r,\theta,z) = \frac{1}{\sqrt{2\pi}} \sum_{|k|\le\mathcal{K}} \boldsymbol{u}^k(r,z) e^{ik\theta}, \quad \breve{p}_{\mathcal{K}}(r,\theta,z) = \frac{1}{\sqrt{2\pi}} \sum_{|k|\le\mathcal{K}} p^k(r,z) e^{ik\theta}. \tag{2.10}$$

The following three-dimensional error between $(\breve{\boldsymbol{u}}, \breve{p})$ and its truncated Fourier series $(\breve{\boldsymbol{u}}_{\mathcal{K}}, \breve{p}_{\mathcal{K}})$ is evaluated in appropriate norms see [5, Thm. 3.1]:

Theorem 2.5. *Let s be a nonnegative real number and assume that the data*

$$(\breve{\boldsymbol{f}}, \breve{p}_b, \breve{\boldsymbol{u}}_0, \breve{g}) \in L^2(0,T;H^{0,s}(\breve{\Omega})^3) \times L^2(0,t;H^{\frac{1}{2},s}(\breve{\Gamma}_P)) \times H^{0,s}(\breve{\Omega})^3 \times H^1(0,t;H^{-1,s}(\breve{\Omega}) \cap H^{-1}_{1\diamond}(\breve{\Omega})).$$

Then, the following bound holds between the solution $(\breve{\boldsymbol{u}}, \breve{p})$ to problem (1.1) and its truncated Fourier series $(\breve{\boldsymbol{u}}_{\mathcal{K}}, \breve{p}_{\mathcal{K}})$:

$$\|\breve{\boldsymbol{u}} - \breve{\boldsymbol{u}}_{\mathcal{K}}\|_{H^1(0,T;L^2(\breve{\Omega})^3)} + \|\breve{p} - \breve{p}_{\mathcal{K}}\|_{L^2(0,T;H^1(\breve{\Omega}))} \le \mathcal{K}^{-s}\Big(\|\breve{\boldsymbol{u}}_0\|_{H^{0,s}(\breve{\Omega})^3} + \|\breve{\boldsymbol{f}}\|_{L^2(0,T;H^{0,s}(\breve{\Omega})^3)} + \|\breve{p}_b\|_{L^2(0,t;H^{\frac{1}{2},s}(\breve{\Gamma}_P))} + \|\breve{g}\|_{H^1(0,t;H^{-1,s}(\breve{\Omega})\cap H^{-1}_{1\diamond}(\breve{\Omega}))}\Big).$$

3. The discrete problem

We split the discretization into two steps: first a semi-discretization in time, and next the full discretization. At each step, we write the variational formulation and we recall the error arising from Fourier truncation.

3.1. The time semi-discrete problem

We introduce a partition of the interval $[0,T]$ into subintervals $[t_{n-1}, t_n]$, $1 \le n \le N$, such that $0 = t_0 < t_1 < \cdots < t_N = T$. We denote by τ_n the time step $t_n - t_{n-1}$, by τ the N-tuple $(\tau_1, \tau_2, \ldots, \tau_N)$ and by $|\tau|$ the maximum of the τ_n, $1 \le n \le N$. The time discretization of problem (2.3)–(2.5) relies on the use of a backward Euler scheme. Thus for all $k \in \mathbb{Z}$, for any data $(\boldsymbol{f}^k, p_b^k) \in C^0(0,T;L^2_1(\Omega)^3) \times C^0(0,T;H^{\frac{1}{2}}_{(k)}(\Gamma_p))$, $g^k \in C^0(0,T;L^2_1(\Gamma_u))$ and $\boldsymbol{u}_0^k \in L^2_1(\Omega)^3$, satisfying $\mathrm{div}_k \boldsymbol{u}_0^k = 0$ in Ω, we consider the following scheme:

Find $(\boldsymbol{u}^{kn})_{0\le n\le N} \in (L^2_1(\Omega)^3)^{N+1}$ and $(p^{kn})_{1\le n\le N} \in (H^1_{(k)}(\Omega))^N$ such that

$$\boldsymbol{u}^{k0} = \boldsymbol{u}_0^k \quad \text{in } \Omega, \tag{3.1}$$

for all n, $1 \le n \le N$,

$$p^{kn} = p_b^{kn} \quad \text{on } \Gamma_p, \tag{3.2}$$

$\forall \boldsymbol{v} \in L^2_1(\Omega)^3$ and $\forall q \in H^1_{(k)\diamond}(\Omega)$,

$$\begin{aligned}(\boldsymbol{u}^{kn}, \overline{\boldsymbol{v}})_1 + \alpha\, \tau_n(\boldsymbol{u}^{kn}, \overline{\boldsymbol{v}})_1 &= (\boldsymbol{u}^{k,n-1}, \overline{\boldsymbol{v}})_1 - \tau_n(\overline{\boldsymbol{v}}, \mathbf{grad}_k p^{kn})_1 + \tau_n(\boldsymbol{f}^{kn}, \overline{\boldsymbol{v}})_1, \\ \overline{b_1^k}(\boldsymbol{u}^{kn}, q) &= \langle g^{kn}, q\rangle_{\Gamma_u},\end{aligned} \tag{3.3}$$

where $\boldsymbol{f}^{kn} = \boldsymbol{f}^k(\cdot, t_n)$, $g^{kn} = g^k(\cdot, t_n)$ and $p_b^{kn} = p_b^k(\cdot, t_n)$. We refer to [5, Sec. 3.1] for the well-posedness of problem (3.1)–(3.3) and its a priori analysis.

Definition 3.1. With each $(\boldsymbol{f}^{kn}, p_b^{kn}, g^{kn}, \boldsymbol{u}_0^k)$, we associate the unique solution $(\boldsymbol{u}^{kn}, p^{kn})$ of problem (3.1)–(3.3), and we define the three-dimensional functions $\breve{\boldsymbol{u}}^n$ and $\breve{p}^n$ by

$$\breve{\boldsymbol{u}}^n(r,\theta,z) = \frac{1}{\sqrt{2\pi}} \sum_{k\in\mathbb{Z}} \boldsymbol{u}^{kn}(r,z)e^{ik\theta}, \quad \breve{p}^n(r,\theta,z) = \frac{1}{\sqrt{2\pi}} \sum_{k\in\mathbb{Z}} p^{kn}(r,z)e^{ik\theta}.$$

We fix the nonnegative integer $\mathcal{K}$ and we introduce the pair $(\breve{\boldsymbol{u}}^n_{\mathcal{K}}, \breve{p}^n_{\mathcal{K}})$ which is obtained from $(\breve{\boldsymbol{u}}^n, \breve{p}^n)$ by Fourier truncation:

$$\breve{\boldsymbol{u}}^n_{\mathcal{K}}(r,\theta,z) = \frac{1}{\sqrt{2\pi}} \sum_{|k|\le\mathcal{K}} \boldsymbol{u}^{kn}(r,z)e^{ik\theta}, \breve{p}^n_{\mathcal{K}}(r,\theta,z) = \frac{1}{\sqrt{2\pi}} \sum_{|k|\le\mathcal{K}} p^{kn}(r,z)e^{ik\theta}. \tag{3.4}$$

Then, the following three-dimensional error between $(\breve{\boldsymbol{u}}^n, \breve{p}^n)$ and its truncated Fourier series $(\breve{\boldsymbol{u}}^n_{\mathcal{K}}, \breve{p}^n_{\mathcal{K}})$ is obtained in [5, Prop. 3.1]:

Proposition 3.2. *Let s be a nonnegative real number and assume that the data*

$$(\breve{\boldsymbol{f}}, \breve{p}_b, \breve{\boldsymbol{u}}_0, \breve{g}) \text{ belong to } C^0(0,T;H^{0,s}(\breve{\Omega})^3) \times C^0(0,t;H^{\frac{1}{2},s}(\breve{\Gamma}_P)) \times H^{0,s}(\breve{\Omega})^3 \times C^0(0,t;H^{-1,s}(\breve{\Omega}) \cap H^{-1}_{1\diamond}(\breve{\Omega})).$$

Then the following estimates hold

$$\|\breve{\boldsymbol{u}}^n - \breve{\boldsymbol{u}}^n_{\mathcal{K}}\|_{L^2(\breve{\Omega})^3} \lesssim \mathcal{K}^{-s}\Big(\|\breve{\boldsymbol{u}}_0\|_{H^{0,s}(\breve{\Omega})^3} + \|\breve{g}(\cdot,0)\|_{H^{-1,s}(\breve{\Omega})\cap H^{-1}_{1\diamond}(\breve{\Omega})} + \|\breve{g}^n\|_{H^{-1,s}(\breve{\Omega})\cap H^{-1}_{1\diamond}(\breve{\Omega})} + \big(\sum_{m=1}^{n}\tau_m\big(\|\breve{\boldsymbol{f}}^m\|^2_{H^{0,s}(\breve{\Omega})^3} + \|\breve{p}^m_b\|^2_{H^{\frac12,s}(\breve{\Gamma}_P)}\big)\big)^{\frac12}\Big),$$

$$\Big(\sum_{m=1}^{n}\tau_m\|\breve{p}^m - \breve{p}^m_{\mathcal{K}}\|^2_{H^1(\breve{\Omega})}\Big)^{\frac12} \lesssim \mathcal{K}^{-s}\Big(\|\breve{\boldsymbol{u}}_0\|_{H^{0,s}(\breve{\Omega})^3} + \|\breve{g}(\cdot,0)\|_{H^{-1,s}(\breve{\Omega})\cap H^{-1}_{1\diamond}(\breve{\Omega})} + \big(\sum_{m=1}^{n}\tau_m\big(\|\breve{\boldsymbol{f}}^m\|^2_{H^{0,s}(\breve{\Omega})^3} + \|\breve{p}^m_b\|^2_{H^{\frac12,s}(\breve{\Gamma}_P)} + \|\breve{g}^m\|^2_{H^{-1,s}(\breve{\Omega})\cap H^{-1}_{1\diamond}(\breve{\Omega})}\big)^{\frac12}\big) + \big(\sum_{m=1}^{n}\tau_m\Big\|\frac{\breve{g}^m - \breve{g}^{m-1}}{\tau_m}\Big\|^2_{H^{-1,s}(\breve{\Omega})\cap H^{-1}_{1\diamond}(\breve{\Omega})}\big)^{\frac12}\Big)$$

and

$$\left(\sum_{m=1}^{n}\tau_m\left\|\frac{(\breve{\boldsymbol{u}}^m - \breve{\boldsymbol{u}}^m_{\mathcal{K}}) - (\breve{\boldsymbol{u}}^{m-1} - \breve{\boldsymbol{u}}^{m-1}_{\mathcal{K}})}{\tau_m}\right\|^2_{L^2(\breve{\Omega})^3}\right)^{\frac12} \lesssim \mathcal{K}^{-s}\Big(\|\breve{\boldsymbol{u}}_0\|_{H^{0,s}(\breve{\Omega})^3} + \|\breve{g}(\cdot,0)\|_{H^{-1,s}(\breve{\Omega})\cap H^{-1}_{1\diamond}(\breve{\Omega})} + \big(\sum_{m=1}^{n}\tau_m\big(\|\breve{\boldsymbol{f}}^m\|^2_{H^{0,s}(\breve{\Omega})^3} + \|\breve{p}^m_b\|^2_{H^{\frac12,s}(\breve{\Gamma}_P)}\big)\big)^{\frac12} + \big(\sum_{m=1}^{n}\tau_m\Big\|\frac{\breve{g}^m - \breve{g}^{m-1}}{\tau_m}\Big\|^2_{H^{-1,s}(\breve{\Omega})\cap H^{-1}_{1\diamond}(\breve{\Omega})}\big)^{\frac12}\Big).$$

3.2. The time and space discrete problem

We now describe the space discretization of problem (3.1)–(3.3). For each n, $0 \le n \le N$, let $(\mathcal{T}_{nh})_h$ be a regular family of triangulations of Ω by closed triangles, in the usual sense, such that:

- for each h, $\overline{\Omega}$ is the union of all elements of $\mathcal{T}_{nh}$,
- both $\overline{\Gamma}_p$ and $\overline{\Gamma}_u$ are the union of whole edges of elements of $\mathcal{T}_{nh}$,
- there exists a constant $\sigma > 0$ independent of h, n and T such that, for all T in $\mathcal{T}_{nh}$, $\frac{h_T}{\rho_T} \le \sigma$, where h_T is the diameter of T, and ρ_T the diameter of its inscribed circle,
- h_n is the maximum of the diameters of the elements of $\mathcal{T}_{nh}$,
- $\mathcal{E}_{nh}$ is the set of all edges e of elements T of $\mathcal{T}_{nh}$,
- $\mathcal{E}^0_{nh}$ is the subset of $\mathcal{E}_{nh}$ whose elements are not contained in $\partial\Omega$,
- $\mathcal{V}_{nh}$ is the set of vertices of the elements of $\mathcal{T}_{nh}$,
- $\mathcal{V}^0_{nh}$ is the subset of $\mathcal{V}_{nh}$ whose elements are inside Ω,
- $\mathcal{V}^b_{nh} = \mathcal{V}_{nh} \setminus \mathcal{V}^0_{nh}$ is the subset of $\mathcal{V}_{nh}$ made of boundary vertices.

For each triangle T and nonnegative integer ℓ, we denote by $P_\ell(T)$ the space of restrictions to T of polynomials with degree $\le \ell$. At each time step, the discrete space of velocities is: $X_{nh}(\Omega) = \{\boldsymbol{v}_h \in L^2_1(\Omega)^3;\ \forall T \in \mathcal{T}_{nh},\ \boldsymbol{v}_h|_T \in P_0(T)^3\}$, its interpolation operator is the orthogonal projection operator Π_{nh} from $L^2_1(\Omega)^3$ onto $X_{nh}(\Omega)$ associated with the scalar product of $L^2_1(\Omega)^3$ and verifies, for every $0 \le s \le 1$

$$\forall \boldsymbol{v} \in H^s_{(k)}(\Omega)^3, \quad \|\boldsymbol{v} - \Pi_{nh}\boldsymbol{v}\|_{L^2_1(\Omega)^3} \lesssim h^s_n\,\|\boldsymbol{v}\|_{H^s_{(k)}(\Omega)^3}. \tag{3.5}$$

We assume that the pressure is continuous whence the choice of discrete space as proposed in [13]: $M_{nh(k)}(\Omega) = \{q_h \in H^1_{(k)}(\Omega);\ \forall T \in \mathcal{T}_{nh},\ q_h|_T \in P_1(T)\}$, its degrees of freedom are defined at the nodes of $\mathcal{V}_{nh}$ and its interpolation operator i_{nh} from $H^1_{(k)}(\Omega)$ onto $M_{nh(k)}(\Omega)$ is the standard Lagrange interpolation operator at the nodes of $\mathcal{V}_{nh}$ with values in $M_{nh(k)}(\Omega)$, which satisfies, for every $\frac12 < s \le 1$

$$\forall q \in H^{s+1}_{(k)}(\Omega), \qquad |q - i_{nh}q|_{H^1_{(k)}(\Omega)} \lesssim h^s_n\,\|q\|_{H^{s+1}_{(k)}(\Omega)}. \tag{3.6}$$

Finally, to approximate functions with zero trace on Γ_p, we set

$$M^0_{nh(k)}(\Omega) = \{q_h \in M_{nh(k)}(\Omega);\ q_h = 0 \text{ on } \Gamma_p\}.$$

3.2.1. Variational formulation of the fully discrete problem

For every data $(\boldsymbol{f}^k, p_b^k)_{k\in\mathbb{Z}} \in C^0(0,T;L_1^2(\Omega)^3)\times C^0(0,T;H_{(k)}^{s+\frac{1}{2}}(\Gamma_p))$, $s>\frac{1}{2}$, $g^k\in C^0(0,T;L_1^2(\Gamma_u))$ and $\boldsymbol{u}_0^k\in L_1^2(\Omega)^3$ with divergence free $\mathrm{div}_k\boldsymbol{u}_0^k=0$ in Ω, the discrete problem constructed by the Galerkin method from (3.1)–(3.3) reads:

Find $(\boldsymbol{u}_h^{kn})_{0\le n\le N}\in(X_{nh}(\Omega))^{N+1}$, and $(p_h^{kn})_{1\le n\le N}\in(M_{nh(k)}(\Omega))^N$, such that

$$\boldsymbol{u}_h^{k0}=\Pi_{0h}\boldsymbol{u}^{k0}\quad\text{in }\Omega, \tag{3.7}$$

for all n, $1\le n\le N$,

$$p_h^{kn}=i_{nh}p_b^{kn}\qquad\text{on }\Gamma_p, \tag{3.8}$$

$$\begin{aligned}\forall\boldsymbol{v}_h\in X_{nh}(\Omega),\qquad &(\boldsymbol{u}_h^{kn},\overline{\boldsymbol{v}}_h)_1+\alpha\,\tau_n(\boldsymbol{u}_h^{kn},\overline{\boldsymbol{v}}_h)_1+\tau_n b_1^k(\boldsymbol{v}_h,p_h^{kn})\\ &\qquad=(\boldsymbol{u}_h^{k,n-1},\overline{\boldsymbol{v}}_h)_1+\tau_n(\boldsymbol{f}^{kn},\overline{\boldsymbol{v}}_h)_1,\\ \forall q_h\in M^0_{nh(k)}(\Omega),\qquad &\overline{b_1^k}(\boldsymbol{u}_h^{kn},q_h)=\langle g^{kn},q_h\rangle_{\Gamma_u}.\end{aligned} \tag{3.9}$$

We recall that this problem has a unique solution see [5, Thm. 3.5]. Moreover, $b_1^k(\cdot,\cdot)$ satisfies the following inf–sup condition see [5, Lem. 3.4], for all $k\in\mathbb{Z}$,

$$\forall q_h\in M^0_{nh(k)}(\Omega),\ \sup_{\boldsymbol{v}_h\in X_{nh}(\Omega)}\frac{b_1^k(\boldsymbol{v}_h,q_h)}{\|\boldsymbol{v}_h\|_{L_1^2(\Omega)^3}}\ge|q_h|_{H^1_{(k)}(\Omega)}. \tag{3.10}$$

The analysis of the problem (3.7)–(3.9) and a priori error estimates were best dealt in [5]. Our goal in this article is to propose and analyze a posteriori error estimates for problem (3.7)–(3.9).

Definition 3.3. Once the discrete coefficients $(\boldsymbol{u}_h^{kn},p_h^{kn})$, $|k|\le\mathcal{K}$, are known, we define the three-dimensional discrete solution

$$\begin{aligned}\breve{\boldsymbol{u}}^n_{\mathcal{K},h}(r,\theta,z)&=\frac{1}{\sqrt{2\pi}}\sum_{|k|\le\mathcal{K}}\boldsymbol{u}_h^{kn}(r,z)e^{ik\theta},\\ \breve{p}^n_{\mathcal{K},h}(r,\theta,z)&=\frac{1}{\sqrt{2\pi}}\sum_{|k|\le\mathcal{K}}p_h^{kn}(r,z)e^{ik\theta}.\end{aligned} \tag{3.11}$$

The following three-dimensional error between the solution $(\breve{\boldsymbol{u}}^n,\breve{p}^n)$ and $(\breve{\boldsymbol{u}}^n_{\mathcal{K},h},\breve{p}^n_{\mathcal{K},h})$ is bounded [5, Thm 3.3 and 3.4]:

Theorem 3.4. *For any $\frac{1}{2}<s\le 1$, assume that the data $(\breve{\boldsymbol{f}},\breve{p}_b,\breve{\boldsymbol{u}}_0,\breve{g})$ belong to $C^0(0,T;H^{0,s}(\breve{\Omega})^3)\times C^0(0,t;H^{\frac{1}{2},s}(\breve{\Gamma}_p))\times H^{0,s}(\breve{\Omega})^3\times C^0(0,t;H^{-1,s}(\breve{\Omega})\cap H^{-1}_{1\diamond}(\breve{\Omega}))$, $\boldsymbol{u}_0^k\in H^s_{(k)}(\Omega)^3$ and the solution $(\mathbf{u}^{kn},p^{kn})\in H^s_{(k)}(\Omega)^3\times H^{s+1}_{(k)}(\Omega)$. Then, the following error estimate holds between the solution $(\breve{\boldsymbol{u}}^n,\breve{p}^n)$ and $(\breve{\boldsymbol{u}}^n_{\mathcal{K},h},\breve{p}^n_{\mathcal{K},h})$: for $1\le n\le N$,*

$$\begin{aligned}\left\|\breve{\boldsymbol{u}}^n-\breve{\boldsymbol{u}}^n_{\mathcal{K},h}\right\|_{L^2(\breve{\Omega})^3}\le{}&\Big(\sum_{m=1}^n\tau_m(h_m)^{2s}\left\|\breve{p}^m\right\|^2_{H^{s+1,s}(\breve{\Omega})}\Big)^{\frac{1}{2}}+\sum_{m=0}^n(h_m)^s\left\|\breve{\boldsymbol{u}}^m\right\|_{H^{s,s}(\breve{\Omega})^3}\\ &+\mathcal{K}^{-s}\Big(\left\|\breve{\boldsymbol{u}}_0\right\|_{H^{0,s}(\breve{\Omega})^3}+\left\|\breve{g}(\cdot,0)\right\|_{H^{-1,s}(\breve{\Omega})\cap H^{-1}_{1\diamond}(\breve{\Omega})}+\left\|\breve{g}^n\right\|_{H^{-1,s}(\breve{\Omega})\cap H^{-1}_{1\diamond}(\breve{\Omega})}\\ &+\Big(\sum_{m=1}^n\tau_m\Big(\left\|\breve{\boldsymbol{f}}^m\right\|^2_{H^{0,s}(\breve{\Omega})^3}+\left\|\breve{p}_b^m\right\|^2_{H^{\frac{1}{2},s}(\breve{\Gamma}_p)}\Big)\Big)^{\frac{1}{2}}\Big).\end{aligned}$$

Theorem 3.5. *Assume that all elements of $\mathcal{T}_{n-1,h}$ are contained in elements of $\mathcal{T}_{nh}$. If the assumptions of Theorem 3.4 are satisfied, the following a priori error estimate holds for n, $1\le n\le N$:*

$$\begin{aligned}(\tau_n)^{\frac{1}{2}}\left\|\breve{p}^n-\breve{p}^n_{\mathcal{K},h}\right\|_{H^1(\breve{\Omega})}\le|\tau|^{\frac{1}{2}}\Big(&\Big(\sum_{m=1}^n\tau_m(h_m)^{2s}\left\|\breve{p}^m\right\|^2_{H^{s+1,s}(\breve{\Omega})}\Big)^{\frac{1}{2}}+h_n\left\|\breve{p}^n\right\|_{H^{s+1,s}(\breve{\Omega})}\\ &+\sum_{m=0}^n(h_m)^s\left\|\breve{\boldsymbol{u}}^m\right\|_{H^{s,s}(\breve{\Omega})^3}\Big)+\mathcal{K}^{-s}\Big(\left\|\breve{\boldsymbol{u}}_0\right\|_{H^{0,s}(\breve{\Omega})^3}+\left\|\breve{g}(\cdot,0)\right\|_{H^{-1,s}(\breve{\Omega})\cap H^{-1}_{1\diamond}(\breve{\Omega})}\\ &+\Big(\sum_{m=1}^n\tau_m\Big(\left\|\breve{\boldsymbol{f}}^m\right\|^2_{H^{0,s}(\breve{\Omega})^3}+\left\|\breve{p}_b^m\right\|^2_{H^{\frac{1}{2},s}(\breve{\Gamma}_p)}+\left\|\breve{g}^n\right\|_{H^{-1,s}(\breve{\Omega})\cap H^{-1}_{1\diamond}(\breve{\Omega})}\Big)\Big)^{\frac{1}{2}}\Big)\\ &+\Big(\sum_{m=1}^n\tau_m\left\|\frac{\breve{g}^m-\breve{g}^{m-1}}{\tau_m}\right\|^2_{H^{-1,s}(\breve{\Omega})\cap H^{-1}_{1\diamond}(\breve{\Omega})}\Big)\Big)^{\frac{1}{2}}.\end{aligned}$$

4. A posteriori analysis

For the time and the space discretizations, we describe a family of error indicators and prove its upper and lower bounds for the error.

4.1. The time discretization

We first define the error indicators and write the residual equations. Next, for each value of k, we prove an a posteriori estimate of the error and an upper bound for each indicator. In a final step, we return to the three-dimensional solution. For each integer k, $1 \le n \le N$, we define the time error indicator, see [9] and [14]

$$\eta_n^k = \left(\frac{\tau_n}{3}\right)^{\frac{1}{2}} \|\boldsymbol{u}_h^{kn} - \boldsymbol{u}_h^{k,n-1}\|_{L_1^2(\Omega)^3}. \tag{4.1}$$

Let $\boldsymbol{u}_\tau^k$ denote the function which is continuous, affine on each interval $[t_{n-1}, t_n]$, $1 \le n \le N$, such that $\forall n,\ 0 \le n \le N,\quad \boldsymbol{u}_\tau^k(t_n) = \boldsymbol{u}^{kn}$, and p_τ^k denote the piecewise constant function such that $\forall n,\ 1 \le n \le N,\quad \forall t \in]t_{n-1}, t_n],\quad p_\tau^k(t) = p^k(t_n)$.

We denote by Π_τ the operator which associates with any continuous function $v \in [0, T]$ the piecewise constant function $\Pi_\tau v$ is equal to $v(t_n)$ on each interval $]t_{n-1}, t_n]$, $1 \le n \le N$. Let $\mathcal{L}$ denote a lifting operator, i.e., an operator from $H_{(k)}^{\frac{1}{2}}(\Gamma_p)$ into $H_{(k)}^1(\Omega)$ which is continuous from $H_{(k)}^{s+\frac{1}{2}}(\Gamma_p)$ into $H_{(k)}^{s+1}(\Omega)$ for all $s \ge 0$ (indeed, the trace operator is surjective). Since $p_b^k \in L^2(0, T; H_{(k)}^{\frac{1}{2}}(\Gamma_p))$, we denote by $\tilde{p}_b^k$ the function defined for a.e. t, $0 \le t \le T$, by $\tilde{p}_b^k(t) = \mathcal{L}(p_b^k(t)) \in L^2(0, T; H_{(k)}^1(\Omega))$ and satisfy

$$\left\|\tilde{p}_b^k\right\|_{L^2(0,T;H_{(k)}^1(\Omega))} \le c_0 \left\|p_b^k\right\|_{L^2(0,T;H_{(k)}^{\frac{1}{2}}(\Gamma_p))}. \tag{4.2}$$

Setting $p_*^k = p^k - \tilde{p}_b^k$, we observe that $p_*^k \in L^2(0, T; H_{(k)\diamond}^1(\Omega))$. Then for all t in $]t_{n-1}, t_n]$, the residual equation in variational form reads

$$\forall \boldsymbol{v} \in L_1^2(\Omega)^3,\ (\partial_t(\boldsymbol{u}^k - \boldsymbol{u}_\tau^k), \overline{\boldsymbol{v}})_1 + \alpha(\boldsymbol{u}^k - \boldsymbol{u}_\tau^k, \overline{\boldsymbol{v}})_1 + b_1^k(\boldsymbol{v}, p_*^k - \Pi_\tau p_*^k)$$
$$= (\boldsymbol{f}^k - \Pi_\tau \boldsymbol{f}^k, \overline{\boldsymbol{v}})_1 - \alpha(\boldsymbol{u}_\tau^k - \boldsymbol{u}^{kn}, \overline{\boldsymbol{v}})_1 - b_1^k(\boldsymbol{v}, \tilde{p}_b^k - \Pi_\tau \tilde{p}_b^k), \tag{4.3}$$

$$\forall q \in H_{(k)\diamond}^1(\Omega),\ \overline{b_1^k}(\boldsymbol{u}^k - \boldsymbol{u}_\tau^k, q) = \left\langle g^k - \Pi_\tau g^k, q\right\rangle_{\Gamma_u}. \tag{4.4}$$

Because of the inf–sup condition (2.7), see [12, Chap. I, Lem. 4.1], we can find a unique $\boldsymbol{u}_b^k \in \mathbb{V}_k(\Omega)^\perp$ such that $\forall q \in H_{(k)\diamond}^1(\Omega),\quad b(\boldsymbol{u}_b^k, q) = \left\langle g^k, q\right\rangle_{\Gamma_u}$, and

$$\left\|\boldsymbol{u}_b^k(\cdot, t)\right\|_{L_1^2(\Omega)^3} \le c \left\|g^k(\cdot, t)\right\|_{L_1^2(\Gamma_u)}. \tag{4.5}$$

Note that the nonnegative constants c_0 and c only depend on Ω. When setting $\boldsymbol{u}_\diamond^k = \boldsymbol{u}^k - \boldsymbol{u}_b^k$ and $\boldsymbol{u}_\diamond^{kn} = \boldsymbol{u}^{kn} - \boldsymbol{u}_b^{kn}$ where $\boldsymbol{u}_b^{kn} = \boldsymbol{u}_b^k(\cdot, t_n)$, we observe that $\boldsymbol{u}_\diamond^k$ and $\boldsymbol{u}_\diamond^{kn}$ belong to $H^1(0, T; \mathbb{V}_k(\Omega))$. Moreover, the residual equations (4.3) and (4.4) are equivalent to:

$$\forall \boldsymbol{v} \in \mathbb{V}_k(\Omega),\ (\partial_t(\boldsymbol{u}_\diamond^k - \boldsymbol{u}_{\diamond\tau}^k), \overline{\boldsymbol{v}})_1 + \alpha(\boldsymbol{u}_\diamond^k - \boldsymbol{u}_{\diamond\tau}^k, \overline{\boldsymbol{v}})_1$$
$$= (\boldsymbol{f}^k - \Pi_\tau \boldsymbol{f}^k, \overline{\boldsymbol{v}})_1 - \alpha(\boldsymbol{u}_{\diamond\tau}^k - \boldsymbol{u}_\diamond^{kn}, \overline{\boldsymbol{v}})_1 - b_1^k(\boldsymbol{v}, \tilde{p}_b^k - \Pi_\tau \tilde{p}_b^k). \tag{4.6}$$

4.1.1. The reliability of the indicator

In this section, we will prove the upper bound of the error. To do so, we first start by introducing the following regularity parameter

$$\sigma_\tau = \max_{1 \le n \le N} \frac{\tau_n}{\tau_{n-1}}, \qquad \text{where} \qquad \tau_0 = \tau_1.$$

Next, we show the error estimate in L^2−norm at t_n for all $1 \le n \le N$:

Proposition 4.1. *The following a posteriori error estimate holds*

$$\left\|\boldsymbol{u}^k(\cdot, t_n) - \boldsymbol{u}^{kn}\right\|_{L_1^2(\Omega)^3} \lesssim \sqrt{\alpha} \left(\sum_{m=1}^n (\eta_m^k)^2\right)^{\frac{1}{2}}$$
$$+ \sqrt{\frac{1}{\alpha}} \left(\left\|\boldsymbol{f}^k - \Pi_\tau \boldsymbol{f}^k\right\|_{L^2(0,t_n;L_1^2(\Omega)^3)} + c_0 \left\|p_b^k - \Pi_\tau p_b^k\right\|_{L^2(0,t_n;H_{(k)}^{\frac{1}{2}}(\Gamma_p))} \right)$$
$$+ \sqrt{\alpha}(1 + \sqrt{\sigma_\tau}) \left(\sum_{m=0}^n \tau_m \left\|\boldsymbol{u}^{km} - \boldsymbol{u}_h^{km}\right\|_{L_1^2(\Omega)^3}^2\right)^{\frac{1}{2}}. \tag{4.7}$$

Proof. Taking $\boldsymbol{v} = \boldsymbol{u}_\diamond^k - \boldsymbol{u}_{\diamond\tau}^k$ in (4.6) yields

$$\frac{1}{2}\frac{d}{dt}\left\|\boldsymbol{u}_\diamond^k - \boldsymbol{u}_{\diamond\tau}^k\right\|^2_{L_1^2(\Omega)^3} + \alpha\left\|\boldsymbol{u}_\diamond^k - \boldsymbol{u}_{\diamond\tau}^k\right\|^2_{L_1^2(\Omega)^3} \le \left(\left\|\boldsymbol{f}^k - \Pi_\tau\boldsymbol{f}^k\right\|_{L_1^2(\Omega)^3} + \left|\tilde{p}_b^k - \Pi_\tau\tilde{p}_b^k\right|_{H^1_{(k)}(\Omega)} + \alpha\left\|\boldsymbol{u}_{\diamond\tau}^k - \boldsymbol{u}_\diamond^{kn}\right\|_{L_1^2(\Omega)^3}\right)\left\|\boldsymbol{u}_\diamond^k - \boldsymbol{u}_{\diamond\tau}^k\right\|_{L_1^2(\Omega)^3},$$

whence

$$\frac{d}{dt}\left\|\boldsymbol{u}_\diamond^k - \boldsymbol{u}_{\diamond\tau}^k\right\|^2_{L_1^2(\Omega)^3} + \alpha\left\|\boldsymbol{u}_\diamond^k - \boldsymbol{u}_{\diamond\tau}^k\right\|^2_{L_1^2(\Omega)^3} \lesssim \alpha\left\|\boldsymbol{u}_{\diamond\tau}^k - \boldsymbol{u}_\diamond^{kn}\right\|^2_{L_1^2(\Omega)^3} + \frac{1}{\alpha}\left(\left\|\boldsymbol{f}^k - \Pi_\tau\boldsymbol{f}^k\right\|^2_{L_1^2(\Omega)^3} + \left|\tilde{p}_b^k - \Pi_\tau\tilde{p}_b^k\right|^2_{H^1_{(k)}(\Omega)}\right).$$

Integrating this inequality between 0 and t_n, using the fact that $(\boldsymbol{u}_\diamond^k - \boldsymbol{u}_{\diamond\tau}^k)(0) = 0$ and $\boldsymbol{u}_\diamond^{kn} = \boldsymbol{u}_{\diamond\tau}^k(t_n) = \Pi_\tau\boldsymbol{u}_{\diamond\tau}^k(t)$ obtain

$$\left\|\boldsymbol{u}_\diamond^k(\cdot, t_n) - \boldsymbol{u}_\diamond^{kn}\right\|^2_{L_1^2(\Omega)^3} \lesssim \alpha\left\|\boldsymbol{u}_{\diamond\tau}^k - \Pi_\tau\boldsymbol{u}_{\diamond\tau}^k\right\|^2_{L^2(0,t_n;L_1^2(\Omega)^3)} + \frac{1}{\alpha}\left(\left\|\boldsymbol{f}^k - \Pi_\tau\boldsymbol{f}^k\right\|^2_{L^2(0,t_n;L_1^2(\Omega)^3)} + \left\|\tilde{p}_b^k - \Pi_\tau\tilde{p}_b^k\right\|^2_{L^2(0,t_n;H^1_{(k)}(\Omega))}\right).$$

The triangle inequality, the fact that $\boldsymbol{u}_\diamond^k = \boldsymbol{u}^k - \boldsymbol{u}_b^k$, $\Pi_\tau\boldsymbol{u}_{b\tau}^k(t) = \boldsymbol{u}_b^{kn} = \boldsymbol{u}_{b\tau}^k(t)$ and estimate (4.2) give us

$$\left\|\boldsymbol{u}^k(\cdot, t_n) - \boldsymbol{u}^{kn}\right\|^2_{L_1^2(\Omega)^3} \lesssim \alpha\left\|(\boldsymbol{u}_\tau^k - \Pi_\tau\boldsymbol{u}_\tau^k)\right\|^2_{L^2(0,t_n;L_1^2(\Omega)^3)} + \frac{1}{\alpha}\left(\left\|\boldsymbol{f}^k - \Pi_\tau\boldsymbol{f}^k\right\|^2_{L^2(0,t_n;L_1^2(\Omega)^3)} + c_0\left\|p_b^k - \Pi_\tau p_b^k\right\|^2_{L^2(0,t_n;H^{\frac{1}{2}}_{(k)}(\Gamma_p))}\right). \tag{4.8}$$

To estimate the first term on the right-hand side, we observe that on the interval $]t_{n-1}, t_n]$, $(\boldsymbol{u}_\tau^k - \Pi_\tau\boldsymbol{u}_\tau^k)(t)$ coincide with $-\frac{t_n - t}{\tau_n}(\boldsymbol{u}^{kn} - \boldsymbol{u}^{k,n-1})$. Thus by integrating this equality between t_{n-1} and t_n and using the fact that $\tau_n = t_n - t_{n-1}$, we obtain

$$\left\|\boldsymbol{u}_\tau^k - \Pi_\tau\boldsymbol{u}_\tau^k\right\|^2_{L^2(t_{n-1},t_n;L_1^2(\Omega)^3)} = \left\|\boldsymbol{u}^{kn} - \boldsymbol{u}^{k,n-1}\right\|^2_{L_1^2(\Omega)^3}\int_{t_{n-1}}^{t_n}\left(\frac{t_n - t}{\tau_n}\right)^2 dt,$$

then

$$\left\|\boldsymbol{u}_\tau^k - \Pi_\tau\boldsymbol{u}_\tau^k\right\|_{L^2(t_{n-1},t_n;L_1^2(\Omega)^3)} = \left(\frac{\tau_n}{3}\right)^{\frac{1}{2}}\left\|\boldsymbol{u}^{kn} - \boldsymbol{u}^{k,n-1}\right\|_{L_1^2(\Omega)^3}. \tag{4.9}$$

On the other hand, the triangle inequality implies

$$\left\|\boldsymbol{u}^{kn} - \boldsymbol{u}^{k,n-1}\right\|_{L_1^2(\Omega)^3} \le \left\|\boldsymbol{u}^{kn} - \boldsymbol{u}_h^{kn}\right\|_{L_1^2(\Omega)^3} + \left\|\boldsymbol{u}_h^{kn} - \boldsymbol{u}_h^{k,n-1}\right\|_{L_1^2(\Omega)^3} + \left\|\boldsymbol{u}_h^{k,n-1} - \boldsymbol{u}^{k,n-1}\right\|_{L_1^2(\Omega)^3}.$$

Multiplying this inequality by $\left(\frac{\tau_n}{3}\right)^{\frac{1}{2}}$ and using the expression of the error indicator (4.1), we find

$$\left(\frac{\tau_n}{3}\right)^{\frac{1}{2}}\left\|\boldsymbol{u}^{kn} - \boldsymbol{u}^{k,n-1}\right\|_{L_1^2(\Omega)^3} \le \left(\frac{\tau_n}{3}\right)^{\frac{1}{2}}\left\|\boldsymbol{u}^{kn} - \boldsymbol{u}_h^{kn}\right\|_{L_1^2(\Omega)^3} + \eta_n^k + \left(\frac{\tau_n}{3}\right)^{\frac{1}{2}}\left\|\boldsymbol{u}_h^{k,n-1} - \boldsymbol{u}^{k,n-1}\right\|_{L_1^2(\Omega)^3}. \tag{4.10}$$

Thus we obtain

$$\left\|\boldsymbol{u}_\tau^k - \Pi_\tau\boldsymbol{u}_\tau^k\right\|_{L^2(t_{n-1},t_n;L_1^2(\Omega)^3)} \le \left(\frac{\tau_n}{3}\right)^{\frac{1}{2}}\left\|\boldsymbol{u}^{kn} - \boldsymbol{u}_h^{kn}\right\|_{L_1^2(\Omega)^3} + \eta_n^k + \left(\frac{\tau_{n-1}}{3}\right)^{\frac{1}{2}}(\sigma_\tau)^{\frac{1}{2}}\left\|\boldsymbol{u}_h^{k,n-1} - \boldsymbol{u}^{k,n-1}\right\|_{L_1^2(\Omega)^2}.$$

Summing over n with $1 \le n \le N$ the square of this inequality, we obtain

$$\left\|\boldsymbol{u}_\tau^k - \Pi_\tau\boldsymbol{u}_\tau^k\right\|^2_{L^2(0,t_n;L_1^2(\Omega)^3)} \lesssim 2\sum_{m=1}^{n}(\eta_m^k)^2 + (1 + \sigma_\tau)\sum_{m=0}^{n}\tau_m\left\|\boldsymbol{u}^{km} - \boldsymbol{u}_h^{km}\right\|^2_{L_1^2(\Omega)^3}. \tag{4.11}$$

Finally by substituting (4.11) in (4.8) we obtain the desired a posteriori error estimate. □

Proposition 4.2. *The following a posteriori error estimate holds*

$$\left\|\partial_t(\boldsymbol{u}^k-\boldsymbol{u}^k_\tau)\right\|_{L^2(0,t_n;L^2_1(\Omega)^3)} \lesssim \left\|\boldsymbol{f}^k-\Pi_\tau\boldsymbol{f}^k\right\|_{L^2(0,t_n;L^2_1(\Omega)^3)} + \left\|g^k-\Pi_\tau g^k\right\|_{H^1(0,t_n;L^2_1(\Gamma_u))} + \left(\sum_{m=1}^{n}(\eta^k_m)^2\right)^{\frac12} + c_0\left\|p^k_b-\Pi_\tau p^k_b\right\|_{L^2(0,t_n;H^{\frac12}_{(k)}(\Gamma_p))} + (1+\sqrt{\sigma_\tau})\left(\sum_{m=0}^{n}\tau_m\left\|\boldsymbol{u}^{km}-\boldsymbol{u}^{km}_h\right\|^2_{L^2_1(\Omega)^3}\right)^{\frac12}. \tag{4.12}$$

Proof. We take $\boldsymbol{v}$ equal to $\partial_t(\boldsymbol{u}^k_\diamond-\boldsymbol{u}^k_{\diamond\tau})$ in (4.6) and apply the Cauchy–Schwarz inequality to obtain

$$\frac12\left\|\partial_t(\boldsymbol{u}^k_\diamond-\boldsymbol{u}^k_{\diamond\tau})\right\|^2_{L^2_1(\Omega)^3}+\frac{\alpha}{2}\frac{d}{dt}\left\|\boldsymbol{u}^k_\diamond-\boldsymbol{u}^k_{\diamond\tau}\right\|^2_{L^2_1(\Omega)^3} \le \left\|\boldsymbol{f}^k-\Pi_\tau\boldsymbol{f}^k\right\|^2_{L^2_1(\Omega)^3} + \alpha^2\left\|\boldsymbol{u}^k_{\diamond\tau}-\Pi_\tau\boldsymbol{u}^k_{\diamond\tau}\right\|^2_{L^2_1(\Omega)^3}+\left\|\tilde p^k_b-\Pi_\tau\tilde p^k_b\right\|^2_{H^1_{(k)}(\Omega)}.$$

Integrating between 0 and t_n, using estimate (4.2) and the fact that $(\boldsymbol{u}^k_\diamond-\boldsymbol{u}^k_{\diamond\tau})(0)=0$, yield

$$\begin{aligned}&\left\|\partial_t(\boldsymbol{u}^k_\diamond-\boldsymbol{u}^k_{\diamond\tau})\right\|^2_{L^2(0,t_n;L^2_1(\Omega)^3)}+\alpha\left\|(\boldsymbol{u}^k_\diamond-\boldsymbol{u}^k_{\diamond\tau})(t_n)\right\|^2_{L^2_1(\Omega)^3}\\ &\le 2\Big(\left\|\boldsymbol{f}^k-\Pi_\tau\boldsymbol{f}^k\right\|^2_{L^2(0,t_n;L^2_1(\Omega)^3)}\\ &\quad+\alpha^2\left\|\boldsymbol{u}^k_{\diamond\tau}-\Pi_\tau\boldsymbol{u}^k_{\diamond\tau}\right\|^2_{L^2(0,t_n;L^2_1(\Omega)^3)}+c_0^2\left\|p^k_b-\Pi_\tau p^k_b\right\|^2_{L^2(0,t_n;H^{\frac12}_{(k)}(\Gamma_p))}\Big).\end{aligned}$$

The triangle inequality and the fact that $\boldsymbol{u}^k_\diamond=\boldsymbol{u}^k-\boldsymbol{u}^k_b$ give us

$$\begin{aligned}&\left\|\partial_t(\boldsymbol{u}^k-\boldsymbol{u}^k_\tau)\right\|^2_{L^2(0,t_n;L^2_1(\Omega)^3)}\\ &\le 2\Big(\left\|\boldsymbol{f}^k-\Pi_\tau\boldsymbol{f}^k\right\|^2_{L^2(0,t_n;L^2_1(\Omega)^3)}+\alpha^2\left\|\boldsymbol{u}^k_\tau-\Pi_\tau\boldsymbol{u}^k_\tau\right\|^2_{L^2(0,t_n;L^2_1(\Omega)^3)}\\ &\quad+c_0^2\left\|p^k_b-\Pi_\tau p^k_b\right\|^2_{L^2(0,t_n;H^{\frac12}_{(k)}(\Gamma_p))}+\left\|\partial_t(\boldsymbol{u}^k_b-\boldsymbol{u}^k_{b\tau})\right\|^2_{L^2(0,t_n;L^2_1(\Omega)^3)}\Big).\end{aligned}$$

Then, (4.12) follows by combining this estimate with (4.5) and (4.11). □

The last result in this section concerns the error estimate of the pressure.

Proposition 4.3. *The following a posteriori error estimate holds, for* $1\le n\le N$

$$\left\|p^k-p^k_\tau\right\|_{L^2(0,t_n;H^1_{(k)}(\Omega))} \lesssim \left\|\boldsymbol{f}^k-\Pi_\tau\boldsymbol{f}^k\right\|_{L^2(0,t_n;L^2_1(\Omega)^3)} + \left\|g^k-\Pi_\tau g^k\right\|_{H^1(0,t_n;L^2_1(\Gamma_u))} + \left(\sum_{m=1}^{n}(\eta^k_m)^2\right)^{\frac12} + c_0\left\|p^k_b-\Pi_\tau p^k_b\right\|_{L^2(0,t_n;H^{\frac12}_{(k)}(\Gamma_p))} + (1+\sqrt{\sigma_\tau})\left(\sum_{m=0}^{n}\tau_m\left\|\boldsymbol{u}^{km}-\boldsymbol{u}^{km}_h\right\|^2_{L^2_1(\Omega)^3}\right)^{\frac12}. \tag{4.13}$$

Proof. From Eq. (4.6) we have for all $\boldsymbol{v}\in L^2_1(\Omega)^3$,

$$b(\boldsymbol{v},p^k_*-\Pi_\tau p^k_*) = (\partial_t(\boldsymbol{u}^k_\tau-\boldsymbol{u}^k),\boldsymbol{v})_1+\alpha(\boldsymbol{u}^k_\tau-\boldsymbol{u}^k,\boldsymbol{v})_1+b^k_1(\boldsymbol{v},\Pi_\tau\tilde p^k_b-\tilde p^k_b) + (\boldsymbol{f}^k-\Pi_\tau\boldsymbol{f}^k,\boldsymbol{v})_1+\alpha(\boldsymbol{u}^{kn}-\boldsymbol{u}^k_\tau,\boldsymbol{v})_1.$$

The Cauchy–Schwarz inequality and the inf–sup condition (2.7) yield

$$\left\|p^k_*-\Pi_\tau p^k_*\right\|_{H^1_{(k)}(\Omega)} \lesssim \left\|\partial_t(\boldsymbol{u}^k_\tau-\boldsymbol{u}^k)\right\|_{L^2_1(\Omega)^3}+\alpha\left\|\boldsymbol{u}^k_\tau-\boldsymbol{u}^k\right\|_{L^2_1(\Omega)^3}+\left\|\tilde p^k_b-\Pi_\tau\tilde p^k_b\right\|_{H^1_{(k)}(\Omega)} + \left\|\boldsymbol{f}^k-\Pi_\tau\boldsymbol{f}^k\right\|_{L^2_1(\Omega)^3}+\alpha\left\|\boldsymbol{u}^{kn}-\boldsymbol{u}^k_\tau\right\|_{L^2_1(\Omega)^3}.$$

Integrating between 0 and t_n, using estimate (4.2) and $\boldsymbol{u}^{kn} = \Pi_\tau \boldsymbol{u}^k_\tau$ we obtain

$$\begin{aligned}&\left\|p^k_* - \Pi_\tau p^k_*\right\|^2_{L^2(0,t_n;H^1_{(k)}(\Omega))}\\ &\lesssim \left\|\partial_t(\boldsymbol{u}^k_\tau - \boldsymbol{u}^k)\right\|^2_{L^2(0,t_n;L^2_1(\Omega)^3)} + c_0^2 \left\|p^k_b - \Pi_\tau p^k_b\right\|^2_{L^2(0,t_n;H^{\frac{1}{2}}_{(k)}(\Gamma_p))}\\ &\quad + \left\|\boldsymbol{f}^k - \Pi_\tau \boldsymbol{f} v\right\|^2_{L^2(0,t_n;L^2_1(\Omega)^3)} + \alpha^2 \left\|\Pi_\tau \boldsymbol{u}^k_\tau - \boldsymbol{u}^k_\tau\right\|^2_{L^2(0,t_n;L^2_1(\Omega)^3)}.\end{aligned}$$

Finally by inserting (4.11) and (4.12) in the last inequality, using the fact that $p^k - p^k_\tau = (p^k_* - \Pi_\tau p^k_*) + (\tilde{p}^k_b - \Pi_\tau \tilde{p}^k_b)$ and the triangle inequality we obtain the desired a posteriori error estimate. □

The last term in (4.7), (4.12) and (4.13), will be afterward evaluated .

4.1.2. The efficiency of the indicator

Concerning the time error indicator $\eta^k_n,\ n = 1, \dots, N$ defined in (4.1), each of them satisfies the following bound:

Proposition 4.4.

$$\begin{aligned}\eta^k_n &\lesssim \left\|\boldsymbol{u}^k - \boldsymbol{u}^k_\tau\right\|_{H^1(t_{n-1},t_n;L^2_1(\Omega)^3)} + \left\|p^k - p^k_\tau\right\|_{L^2(t_{n-1},t_n;H^1_{(k)}(\Omega))}\\ &\quad + \left\|\boldsymbol{f}^k - \Pi_\tau \boldsymbol{f}^k\right\|_{L^2(t_{n-1},t_n;L^2_1(\Omega)^3)} + (1+\sqrt{\sigma_\tau})\Big(\sum_{m=n-1}^{n} \tau_m \left\|\boldsymbol{u}^{km} - \boldsymbol{u}^{km}_h\right\|^2_{L^2_1(\Omega)^3}\Big)^{\frac{1}{2}}.\end{aligned} \tag{4.14}$$

Moreover this estimate is local with respect to the time variable.

Proof. We easily derive

$$\begin{aligned}\eta^k_n \le &\left(\frac{\tau_n}{3}\right)^{\frac{1}{2}} \left\|\boldsymbol{u}^{kn}_h - \boldsymbol{u}^{kn}\right\|_{L^2_1(\Omega)^3} + \left(\frac{\tau_n}{3}\right)^{\frac{1}{2}} \left\|\boldsymbol{u}^{kn} - \boldsymbol{u}^{k,n-1}\right\|_{L^2_1(\Omega)^3}\\ &+ \left(\frac{\tau_{n-1}}{3}\right)^{\frac{1}{2}} (\sigma_\tau)^{\frac{1}{2}} \left\|\boldsymbol{u}^{k,n-1} - \boldsymbol{u}^{k,n-1}_h\right\|_{L^2_1(\Omega)^3},\end{aligned}$$

then,

$$\begin{aligned}\eta^k_n \lesssim &\left(\frac{\tau_n}{3}\right)^{\frac{1}{2}} \left\|\boldsymbol{u}^{kn} - \boldsymbol{u}^{k,n-1}\right\|_{L^2_1(\Omega)^3}\\ &+ (1+\sqrt{\sigma_\tau})\left(\sum_{m=n-1}^{n} \tau_m \left\|\boldsymbol{u}^{km} - \boldsymbol{u}^{km}_h\right\|^2_{L^2_1(\Omega)^3}\right)^{\frac{1}{2}}.\end{aligned} \tag{4.15}$$

In order to evaluate the first term on the right-hand side, we take $\boldsymbol{v} = \boldsymbol{u}^k_\tau - \boldsymbol{u}^{kn}$ in (4.6) and we use the fact that $p^k_* + \tilde{p}^k_b = p^k$, $\Pi_\tau p^k = p^k_\tau$ and $\boldsymbol{u}^{kn} = \Pi_\tau \boldsymbol{u}^k_\tau$, we obtain

$$\begin{aligned}\left\|\boldsymbol{u}^k_\tau - \Pi_\tau \boldsymbol{u}^k_\tau\right\|^2_{L^2_1(\Omega)^3} \lesssim &\left\|\partial_t(\boldsymbol{u}^k_\tau - \boldsymbol{u}^k)\right\|^2_{L^2_1(\Omega)^3} + \left\|\boldsymbol{u}^k_\tau - \boldsymbol{u}^k\right\|^2_{L^2_1(\Omega)^3}\\ &+ \left\|p^k_\tau - p^k\right\|^2_{H^1_{(k)}(\Omega)} + \left\|\boldsymbol{f}^k - \Pi_\tau \boldsymbol{f}^k\right\|^2_{L^2_1(\Omega)^3}.\end{aligned}$$

Integrating this inequality between t_{n-1} and t_n and using (4.9) yield

$$\begin{aligned}\frac{\tau_n}{3} \left\|\boldsymbol{u}^{kn} - \boldsymbol{u}^{k,n-1}\right\|^2_{L^2_1(\Omega)^3} \lesssim &\left\|\boldsymbol{u}^k_\tau - \boldsymbol{u}^k\right\|^2_{H^1(t_{n-1},t_n;L^2_1(\Omega)^3)}\\ &+ \left\|p^k_\tau - p^k\right\|^2_{L^2(t_{n-1},t_n;H^1_{(k)}(\Omega))} + \left\|\boldsymbol{f}^k - \Pi_\tau \boldsymbol{f}^k\right\|^2_{L^2(t_{n-1},t_n;L^2_1(\Omega)^3)}.\end{aligned}$$

Finally by substituting the previous inequality in (4.15) we obtain the desired estimate. □

4.1.3. The three-dimensional error

We define the three-dimensional functions $(\breve{\boldsymbol{u}}_\tau, \breve{p}_\tau)$ and $(\breve{\boldsymbol{u}}_{\tau\mathcal{K}}, \breve{p}_{\tau\mathcal{K}})$ by

$$\begin{aligned}\breve{\boldsymbol{u}}_\tau(r,\theta,z) &= \frac{1}{\sqrt{2\pi}} \sum_{k\in\mathbb{Z}} \boldsymbol{u}^k_\tau(r,z) e^{ik\theta}, & \breve{p}_\tau(r,\theta,z) &= \frac{1}{\sqrt{2\pi}} \sum_{k\in\mathbb{Z}} p^k_\tau(r,z) e^{ik\theta},\\ \breve{\boldsymbol{u}}_{\tau\mathcal{K}}(r,\theta,z) &= \frac{1}{\sqrt{2\pi}} \sum_{|k|\le\mathcal{K}} \boldsymbol{u}^k_\tau(r,z) e^{ik\theta}, & \breve{p}_{\tau\mathcal{K}}(r,\theta,z) &= \frac{1}{\sqrt{2\pi}} \sum_{|k|\le\mathcal{K}} p^k_\tau(r,z) e^{ik\theta}.\end{aligned} \tag{4.16}$$

Theorem 4.5. *The following estimates hold for any nonnegative real number s*

$$\left\|(\breve{\boldsymbol{u}}(\cdot,t_n)-\breve{\boldsymbol{u}}_{\mathcal{K}}(\cdot,t_n))-(\breve{\boldsymbol{u}}^n-\breve{\boldsymbol{u}}^n_{\mathcal{K}})\right\|_{L^2(\breve{\Omega})^3}\le \mathcal{K}^{-s}\Big(2\alpha\big(\sum_{k\in\mathbb{Z}}(1+|k|^2)^s\sum_{m=1}^{n}(\eta_m^k)^2\big)$$
$$+\frac{1}{\alpha}\big(\left\|\breve{\boldsymbol{f}}-\Pi_\tau\breve{\boldsymbol{f}}\right\|^2_{L^2(0,t_n;H^{0,s}(\breve{\Omega})^3)}+c_0^2\left\|\breve{p}_b-\Pi_\tau\breve{p}_b\right\|^2_{L^2(0,t_n;H^{\frac12,s}(\breve{\Gamma}_p))}\big)$$
$$+\alpha(1+\sigma_\tau)\sum_{m=0}^{n}\tau_m\left\|\breve{\boldsymbol{u}}^m-\breve{\boldsymbol{u}}^m_h\right\|^2_{H^{0,s}(\breve{\Omega})^3}\Big)^{\frac12}$$

and

$$\left\|\partial_t(\breve{\boldsymbol{u}}-\breve{\boldsymbol{u}}_{\mathcal{K}})-\partial_t(\breve{\boldsymbol{u}}_\tau-\breve{\boldsymbol{u}}_{\tau\mathcal{K}})\right\|_{L^2(0,t_n;L^2(\breve{\Omega})^3)}+\left\|(\breve{p}-\breve{p}_{\mathcal{K}})-(\breve{p}_\tau-\breve{p}_{\tau\mathcal{K}})\right\|_{L^2(0,t_n;H^1(\breve{\Omega}))}$$
$$\le\mathcal{K}^{-s}\Big(\left\|\breve{\boldsymbol{f}}-\Pi_\tau\breve{\boldsymbol{f}}\right\|^2_{L^2(0,t_n;H^{0,s}(\breve{\Omega})^3)}+\left\|\breve{p}_b-\Pi_\tau\breve{p}_b\right\|^2_{L^2(0,t_n;;H^{\frac12,s}(\breve{\Gamma}_p))}$$
$$+\big(\sum_{k\in\mathbb{Z}}(1+|k|^2)^s\sum_{m=1}^{n}(\eta_m^k)^2\big)+(1+\sigma_\tau)\sum_{m=0}^{n}\tau_m\left\|\breve{\boldsymbol{u}}^m-\breve{\boldsymbol{u}}^m_h\right\|^2_{H^{0,s}(\breve{\Omega})^3}\Big)^{\frac12}. \tag{4.17}$$

Proof. The definitions of $\breve{\boldsymbol{u}}^n_{\mathcal{K}}$, $\breve{\boldsymbol{u}}_{\tau\mathcal{K}}$ and $\breve{p}_{\tau\mathcal{K}}$ in (3.4) and (4.16) yield

$$\left\|(\breve{\boldsymbol{u}}(\cdot,t_n)-\breve{\boldsymbol{u}}_{\mathcal{K}}(\cdot,t_n))-(\breve{\boldsymbol{u}}^n-\breve{\boldsymbol{u}}^n_{\mathcal{K}})\right\|^2_{L^2(\breve{\Omega})^3}\le\sum_{|k|>\mathcal{K}}\left\|\boldsymbol{u}^k(\cdot,t_n)-\boldsymbol{u}^{kn}\right\|^2_{H^0_{(k)}(\Omega)^3}$$

and

$$\left\|\partial_t(\breve{\boldsymbol{u}}-\breve{\boldsymbol{u}}_{\mathcal{K}})-\partial_t(\breve{\boldsymbol{u}}_\tau-\breve{\boldsymbol{u}}_{\tau\mathcal{K}})\right\|^2_{L^2(\breve{\Omega})^3}+\left\|(\breve{p}-\breve{p}_{\mathcal{K}})-(\breve{p}_\tau-\breve{p}_{\tau\mathcal{K}})\right\|^2_{H^1(\breve{\Omega})}$$
$$\le\sum_{|k|>\mathcal{K}}\left\|\partial_t(\boldsymbol{u}^k-\boldsymbol{u}^k_\tau)\right\|^2_{H^0_{(k)}(\Omega)^3}+\left\|p^k-p^k_\tau\right\|^2_{H^1_{(k)}(\Omega)}.$$

Since $(1+|k|^2)^{-s}<\mathcal{K}^{-2s}$, we obtain

$$\left\|(\breve{\boldsymbol{u}}(\cdot,t_n)-\breve{\boldsymbol{u}}_{\mathcal{K}}(\cdot,t_n))-(\breve{\boldsymbol{u}}^n-\breve{\boldsymbol{u}}^n_{\mathcal{K}})\right\|^2_{L^2(\breve{\Omega})^3}$$
$$\le\mathcal{K}^{-2s}\sum_{k\in\mathbb{Z}}(1+|k|^2)^s\left\|\boldsymbol{u}^k(\cdot,t_n)-\boldsymbol{u}^{kn}\right\|^2_{H^0_{(k)}(\Omega)^3}$$

and

$$\left\|\partial_t(\breve{\boldsymbol{u}}-\breve{\boldsymbol{u}}_{\mathcal{K}})-\partial_t(\breve{\boldsymbol{u}}_\tau-\breve{\boldsymbol{u}}_{\tau\mathcal{K}})\right\|^2_{L^2(\breve{\Omega})^3}+\left\|(\breve{p}-\breve{p}_{\mathcal{K}})-(\breve{p}_\tau-\breve{p}_{\tau\mathcal{K}})\right\|^2_{H^1(\breve{\Omega})}$$
$$\le\mathcal{K}^{-2s}\sum_{k\in\mathbb{Z}}(1+|k|^2)^s\big(\left\|\partial_t(\boldsymbol{u}^k-\boldsymbol{u}^k_\tau)\right\|^2_{H^0_{(k)}(\Omega)^3}+\left\|p^k-p^k_\tau\right\|^2_{H^1_{(k)}(\Omega)}\big).$$

Then (4.17) follows from integrating the last estimate between 0 and t_n, estimates (4.12) and (4.13) and Lemma 2.1. □

4.2. The space discretization

To deal with the fully a posteriori error estimates, we introduce a regular family $(\mathcal{T}_{knh})_h$ of triangulations of Ω which satisfy the assumptions stated in Section 3.2.

For each $T\in\mathcal{T}_{knh}$, we associate

- the set $\mathcal{E}_T$ of edges of T,
- $\mathcal{E}_T^0=\mathcal{E}_T\cap\mathcal{E}^0_{nh}$,
- the diameter h_e of edge e of element T of $\mathcal{T}_{knh}$,
- $\mathcal{E}^{\Gamma_u}_{nh}=\{e\in\mathcal{E}_{nh};\ e\subset\Gamma_u\}$, where $\mathcal{E}^0_{nh}$ and $\mathcal{E}_{nh}$ are defined in Section 3.2.

We are now in a position to introduce the family of error indicators: For each integer k, $-\mathcal{K}\le k\le\mathcal{K}$, each n, $1\le n\le N$ and each triangle T in $\mathcal{T}_{knh}$, we define the following error indicators

$$\eta_T^{kn}=\frac{1}{\tau_n}\left\|\boldsymbol{u}_h^{k,n-1}-\Pi_{nh}\boldsymbol{u}_h^{k,n-1}\right\|_{L^2_1(T)^3}\quad\text{and}\quad\eta_{\partial T}^{kn}=\sum_{e\in\mathcal{E}^{\Gamma_u}_{nh}}h_e^{\frac12}\left\|[\boldsymbol{u}_h^{kn}\cdot\boldsymbol{n}_e]_e\right\|_{L^2_1(e)}. \tag{4.18}$$

Since $\boldsymbol{u}_h^{kn} \in X_{nh}(\Omega)$, the jumps $[\boldsymbol{u}_h^{kn} \cdot \boldsymbol{n}_e]_e$ are constant on each e. Moreover, in the context of mesh adaptivity, the term $\boldsymbol{u}_h^{k,n-1} - \Pi_{nh}\boldsymbol{u}_h^{k,n-1}$ only differs from zero in the elements T of $\mathcal{T}_{knh}$ that are the union of several elements of $\mathcal{T}_{k,n-1,h}$. Therefore these indicators can be readily and explicitly computed.

We approximate the boundary data p_b^{kn} by the Lagrange interpolation operator i_{nh}, with values in $M^0_{nh(k)}(\Omega)$, i.e. for each continuous function $q \in \Gamma_p$, $i_{nh}q$ is a piecewise affine function equal to q on each node of $\mathcal{V}^b_{nh}$.

In order to prove the a posteriori estimates, we first write the residual equations. We recall that $p_*^{kn} = p^{kn} - \tilde{p}_b^{kn}$ and $p_{*h}^{kn} = p_h^{kn} - \mathcal{L}(i_{nh}p_b^{kn})$, where $\tilde{p}_b^{kn} = \mathcal{L}(p_b^{kn})$ and p_{*h}^{kn} is no longer a piecewise polynomial function.

Lemma 4.6. *For any solutions $(\boldsymbol{u}^{kn}, p^{kn})_{1\le n\le N}$ to problem (3.1)–(3.3) and $(\boldsymbol{u}_h^{kn}, p_h^{kn})_{1\le n\le N}$ to problem (3.7)–(3.9), the error $(\boldsymbol{u}^{kn} - \boldsymbol{u}_h^{kn}, p^{kn} - p_h^{kn})_{1\le n\le N}$ satisfies the following residual equations: for all $(\boldsymbol{v}, q) \in L^2_1(\Omega)^3 \times H^1_{(k)\diamond}(\Omega)$*

$$\begin{aligned}
&(\boldsymbol{u}^{kn} - \boldsymbol{u}_h^{kn}, \overline{\boldsymbol{v}})_1 + \alpha\tau_n(\boldsymbol{u}^{kn} - \boldsymbol{u}_h^{kn}, \overline{\boldsymbol{v}})_1 + \tau_n b_1^k(\boldsymbol{v}, p_*^{kn} - p_{*h}^{kn})\\
&= (\boldsymbol{u}^{k,n-1} - \boldsymbol{u}_h^{k,n-1}, \overline{\boldsymbol{v}})_1 + (\boldsymbol{u}_h^{k,n-1} - \Pi_{nh}\boldsymbol{u}_h^{k,n-1}, \overline{\boldsymbol{v}})_1\\
&\qquad + \tau_n(\boldsymbol{f}^{kn} - \Pi_{nh}\boldsymbol{f}^{kn}, \overline{\boldsymbol{v}})_1 - \tau_n b_1^k(\boldsymbol{v}, \mathcal{L}(p_b^{kn} - i_{nh}p_b^{kn})),\\
&\overline{b_1^k}(\boldsymbol{u}^{kn} - \boldsymbol{u}_h^{kn}, q) = \langle g^{kn}, q - q_h^n\rangle_{\Gamma_u}\\
&- \frac{1}{2}\sum_{T\in\mathcal{T}_{knh}}\sum_{e\in\mathcal{E}^{\Gamma_u}_{nh}}\int_e [\boldsymbol{u}_h^{kn}\cdot\boldsymbol{n}_e]_e(\tau)(\overline{q} - \overline{q_h^n})(\tau)d\tau.
\end{aligned} \tag{4.19}$$

Proof. Taking $\boldsymbol{v}_h = \chi_T\,\mathbf{e}$ in the first equation of (3.9), where χ_T is the characteristic function of T and $\mathbf{e}$ runs through the canonical basis of $\mathbb{R}^3$, we obtain for all $T \in \mathcal{T}_{knh}$,

$$(\boldsymbol{u}_h^{kn}, \chi_T\mathbf{e})_1 + \alpha\tau_n(\boldsymbol{u}_h^{kn}, \chi_T\mathbf{e})_1 + \tau_n b_1^k(\chi_T\mathbf{e}, p_h^{kn}) = (\boldsymbol{u}_h^{k,n-1}, \chi_T\mathbf{e})_1 + \tau_n(\boldsymbol{f}^{kn}, \chi_T\mathbf{e})_1.$$

Then

$$\begin{aligned}
\boldsymbol{u}_h^{kn} + \alpha\tau_n\boldsymbol{u}_h^{kn} + \tau_n\mathbf{grad}_k p_h^{kn} &= \boldsymbol{u}_h^{k,n-1} + \frac{\tau_n}{\text{meas}(T)}\int_T \boldsymbol{f}^{kn} r dr dz\\
&= \Pi_{nh}\boldsymbol{u}_h^{k,n-1} + \tau_n\Pi_{nh}\boldsymbol{f}^{kn}.
\end{aligned}$$

Multiplying this equation by any $\overline{\boldsymbol{v}} \in L^2_1(\Omega)^3$, integrating on each $T \in \mathcal{T}_{knh}$, and summing over all elements $T \in \mathcal{T}_{knh}$, we obtain

$$\begin{aligned}
&\sum_{T\in\mathcal{T}_{knh}}\int_T (\boldsymbol{u}_h^{kn} + \alpha\tau_n\boldsymbol{u}_h^{kn} + \tau_n\mathbf{grad}_k p_h^{kn})\cdot\overline{\boldsymbol{v}}\, r dr dz\\
&\quad = \sum_{T\in\mathcal{T}_{knh}}\int_T (\Pi_{nh}\boldsymbol{u}_h^{k,n-1} + \tau_n\Pi_{nh}\boldsymbol{f}^{kn})\cdot\overline{\boldsymbol{v}}\, r dr dz.
\end{aligned}$$

Finally, subtracting this equality from the first equation of (3.3), we obtain the first equation of (4.19). On the other hand, the second equations of (3.3) and (3.9) give $\forall q_h^n \in M^0_{nh(k)}(\Omega)$, $\overline{b_1^k}(\boldsymbol{u}^{kn} - \boldsymbol{u}_h^{kn}, q_h^n) = 0$. Then by Green's formula, we obtain

$$\begin{aligned}
\overline{b_1^k}(\boldsymbol{u}^{kn} - \boldsymbol{u}_h^{kn}, q) &= \overline{b_1^k}(\boldsymbol{u}^{kn} - \boldsymbol{u}_h^{kn}, q - q_h^n),\\
&= \overline{b_1^k}(\boldsymbol{u}^{kn}, q - q_h^n) - \overline{b_1^k}(\boldsymbol{u}_h^{kn}, q - q_h^n)\\
&= \overline{b_1^k}(\boldsymbol{u}^{kn}, q - q_h^n) - b_1^{-k}(\overline{\boldsymbol{u}_h^{kn}}, \overline{q - q_h^n})\\
&= \langle g^{kn}, q - q_h^n\rangle_{\Gamma_u} - \sum_{T\in\mathcal{T}_{knh}}\int_T \boldsymbol{u}_h^{kn}\cdot\mathbf{grad}_{-k}(\overline{q - q_h^n})\, r dr dz\\
&= \langle g^{kn}, q - q_h^n\rangle_{\Gamma_u} - \sum_{T\in\mathcal{T}_{knh}}\int_{\partial T\cap(\Omega\cup\Gamma_u)} (\boldsymbol{u}_h^{kn}\cdot\boldsymbol{n})(\tau)(\overline{q} - \overline{q_h^n})(\tau)\, d\tau,
\end{aligned}$$

whence the second line in (4.19). □

4.3. The reliability of the indicators

For each value of k, we prove an a posteriori estimate of the error. In a final step, we return to the three-dimensional solution.

Proposition 4.7. *The following a posteriori error estimate holds between the solutions $(\boldsymbol{u}^{kn}, p^{kn})_{1\le n\le N}$ to problem (3.1)–(3.3) and $(\boldsymbol{u}_h^{kn}, p_h^{kn})_{1\le n\le N}$ to problem (3.7)–(3.9),*

$$\left\|\boldsymbol{u}^{kn}-\boldsymbol{u}_h^{kn}\right\|^2_{L^2_1(\Omega)^3} \le \left\|\boldsymbol{u}_0^k-\Pi_{0h}\boldsymbol{u}_0^k\right\|^2_{L^2_1(\Omega)^3} + c\Big((G_{kn})^2+\sum_{T\in\mathcal{T}_{knh}}(\eta_{\partial T}^{kn})^2\Big) + \frac{2}{\alpha}\sum_{m=1}^{n}\tau_m\Big(J^2_{km}+\sum_{T\in\mathcal{T}_{knh}}(\eta_T^{km})^2\Big), \tag{4.20}$$

where $J_{kn}=\left\|\boldsymbol{f}^{kn}-\Pi_{nh}\boldsymbol{f}^{kn}\right\|_{L^2_1(\Omega)^3}$ *and* $G_{kn}=\left\|p_b^{kn}-i_{nh}p_b^{kn}\right\|_{H^{\frac12}_{(k)}(\Gamma_p)}$.

Proof. To simplify, let $\boldsymbol{w}^{kn}=\boldsymbol{u}^{kn}-\boldsymbol{u}_h^{kn}$, $r_*^{kn}=p_*^{kn}-p_{*h}^{kn}$ and

$$\boldsymbol{F}^{kn}=\boldsymbol{f}^{kn}-\Pi_{nh}\boldsymbol{f}^{kn}-\mathbf{grad}_k\mathcal{L}(p_b^{kn}-i_{nh}p_b^{kn})+\frac{1}{\tau_n}(\boldsymbol{u}_h^{k,n-1}-\Pi_{nh}\boldsymbol{u}^{k,n-1}).$$

Therefore the residual equations (4.19) become for all $(\boldsymbol{v},q)\in L^2_1(\Omega)^3\times H^1_{(k)\diamond}(\Omega)$

$$\begin{aligned}&(\boldsymbol{w}^{kn},\overline{\boldsymbol{v}})_1+\alpha\tau_n(\boldsymbol{w}^{kn},\overline{\boldsymbol{v}})_1+\tau_n b_1^k(\boldsymbol{v},r_*^{kn})=(\boldsymbol{w}^{k,n-1},\overline{\boldsymbol{v}})_1+\tau_n(\boldsymbol{F}^{kn},\overline{\boldsymbol{v}})_1,\\ &\overline{b_1^k}(\boldsymbol{w}^{kn},q)=\langle g^{kn},q-R_h^nq\rangle_{\Gamma_u}-\frac12\sum_{T\in\mathcal{T}_{nh}}\sum_{e\in\mathcal{E}_{nh}^{\Gamma_u}}\int_e[\boldsymbol{u}_h^{kn}\cdot\boldsymbol{n}_e]_e(\tau)(\overline{q}-\overline{R_h^nq})(\tau)d\tau,\end{aligned} \tag{4.21}$$

where R_h^n denotes a Clément type regularization operator with values in $M^0_{nh(k)}$ such as the Scott and Zhang operator [15]. This operator preserves the zero boundary trace and satisfies for each $T\in\mathcal{T}_{knh}$, and $e\in\mathcal{E}_{nh}^{\Gamma_u}$, see [16, Cor. IX.3.9], [15] and also [17] for the extension to weighted spaces,

$$\forall q\in H^1_{(k)}(\Omega),\ \left\|q-R_h^nq\right\|_{L^2_1(e)}\le ch_e^{\frac12}\left\|q\right\|_{H^1_{(k)}(\Delta_e)},$$

where Δ_e is an appropriate neighborhood of e. Then from this inequality, there exists a unique $\mu^{kn}\in H^1_{(k)\diamond}(\Omega)$ such that for all $q\in H^1_{(k)\diamond}(\Omega)$

$$\begin{aligned}\Big(\overline{\mathbf{grad}_k\mu^{kn}},\mathbf{grad}_kq\Big)_1 &= b_1^k(\boldsymbol{w}^{kn},q)\\ \left|\mu^{kn}\right|_{H^1_{(k)}(\Omega)} &\le c\left(\sum_{T\in\mathcal{T}_{knh}}\sum_{e\in\mathcal{E}_{nh}^{\Gamma_u}}h_e\left\|[\boldsymbol{u}_h^{kn}\cdot\boldsymbol{n}_e]_e\right\|^2_{L^2_1(e)}\right)^{\frac12}.\end{aligned} \tag{4.22}$$

Hence, $\boldsymbol{w}^{kn}$ has the orthogonal decomposition: $\boldsymbol{w}^{kn}=\boldsymbol{w}_*^{kn}+\mathbf{grad}_k\mu^{kn}$, with $\boldsymbol{w}_*^{kn}$ belonging to $\mathbb{V}_k(\Omega)$ (see (2.6)). Taking $\boldsymbol{v}=\boldsymbol{w}_*^{kn}$ in the first equation of problem (4.21), using the fact that $(\boldsymbol{w}^{kn},\overline{\boldsymbol{w}_*^{kn}})_1=\left\|\boldsymbol{w}_*^{kn}\right\|^2_{L^2_1(\Omega)^3}$, $(\boldsymbol{w}^{k,n-1},\overline{\boldsymbol{w}_*^{kn}})_1=(\boldsymbol{w}_*^{k,n-1},\overline{\boldsymbol{w}_*^{kn}})_1$, and the Cauchy–Schwarz inequality we obtain

$$\left\|\boldsymbol{w}_*^{kn}\right\|^2_{L^2_1(\Omega)^3}-(\boldsymbol{w}_*^{k,n-1},\overline{\boldsymbol{w}_*^{kn}})_1+\alpha\tau_n\left\|\boldsymbol{w}_*^{kn}\right\|^2_{L^2_1(\Omega)^3}=\tau_n(\boldsymbol{F}^{kn},\overline{\boldsymbol{w}_*^{kn}})_1.$$

This is equivalent to

$$\left\|\overline{\boldsymbol{w}_*^{kn}}\right\|^2_{L^2_1(\Omega)^3}-(\boldsymbol{w}_*^{k,n-1},\overline{\boldsymbol{w}_*^{kn}})_1+\alpha\tau_n\left\|\overline{\boldsymbol{w}_*^{kn}}\right\|^2_{L^2_1(\Omega)^3}=\tau_n(\boldsymbol{F}^{kn},\overline{\boldsymbol{w}_*^{kn}})_1.$$

Consequently,

$$\frac12\left(\left\|\overline{\boldsymbol{w}_*^{kn}}\right\|^2_{L^2_1(\Omega)^3}-\left\|\boldsymbol{w}_*^{k,n-1}\right\|^2_{L^2_1(\Omega)^3}+\left\|\overline{\boldsymbol{w}_*^{kn}}-\boldsymbol{w}_*^{k,n-1}\right\|^2_{L^2_1(\Omega)^3}\right)+\alpha\tau_n\left\|\overline{\boldsymbol{w}_*^{kn}}\right\|^2_{L^2_1(\Omega)^3} \le \tau_n\left\|\boldsymbol{F}^{kn}\right\|_{L^2_1(\Omega)^3}\left\|\overline{\boldsymbol{w}_*^{kn}}\right\|_{L^2_1(\Omega)^3}.$$

Young's inequality gives

$$\left\|\overline{\boldsymbol{w}_*^{kn}}\right\|^2_{L^2_1(\Omega)^3}-\left\|\boldsymbol{w}_*^{k,n-1}\right\|^2_{L^2_1(\Omega)^3}+\left\|\overline{\boldsymbol{w}_*^{kn}}-\boldsymbol{w}_*^{k,n-1}\right\|^2_{L^2_1(\Omega)^3}+\alpha\tau_n\left\|\overline{\boldsymbol{w}_*^{kn}}\right\|^2_{L^2_1(\Omega)^3} \le \frac{\tau_n}{\alpha}\left\|\boldsymbol{F}^{kn}\right\|^2_{L^2_1(\Omega)^3}.$$

Then

$$\left\|\boldsymbol{w}_*^{kn}\right\|^2_{L^2_1(\Omega)^3} - \left\|\boldsymbol{w}_*^{k,n-1}\right\|^2_{L^2_1(\Omega)^3} \le \frac{\tau_n}{\alpha}\left\|\boldsymbol{F}^{kn}\right\|^2_{L^2_1(\Omega)^3}.$$

Summing this inequality over n yields

$$\left\|\boldsymbol{w}_*^{kn}\right\|^2_{L^2_1(\Omega)^3} - \left\|\boldsymbol{w}_*^{k0}\right\|^2_{L^2_1(\Omega)^3} \le \frac{1}{\alpha}\sum_{m=1}^{n}\tau_m\left\|\boldsymbol{F}^{km}\right\|^2_{L^2_1(\Omega)^3}.$$

Using the fact that $\left\|\boldsymbol{w}^{kn}\right\|^2_{L^2_1(\Omega)^3} = \left|\mu^{kn}\right|^2_{H^1_{(k)}(\Omega)} + \left\|\boldsymbol{w}_*^{kn}\right\|^2_{L^2_1(\Omega)^3}$, we obtain

$$\left\|\boldsymbol{w}^{kn}\right\|^2_{L^2_1(\Omega)^3} \le \left\|\boldsymbol{w}^{k0}\right\|^2_{L^2_1(\Omega)^3} + \left|\mu^{kn}\right|^2_{H^1_{(k)}(\Omega)} + \frac{1}{\alpha}\sum_{m=1}^{n}\tau_m\left\|\boldsymbol{F}^{km}\right\|^2_{L^2_1(\Omega)^3}.$$

Finally by inserting (4.22) into this inequality, using the fact that

$$\left\|\boldsymbol{F}^{kn}\right\|_{L^2_1(\Omega)^3} \le \left\|\boldsymbol{f}^{kn} - \Pi_{nh}\boldsymbol{f}^{kn}\right\|_{L^2_1(\Omega)^3} + \left\|p_b^{kn} - i_{nh}p_b^{kn}\right\|_{H^{\frac{1}{2}}_{(k)}(\Gamma_p)} + \eta_T^{kn},$$

and $\boldsymbol{w}^{kn} = \boldsymbol{u}^{kn} - \boldsymbol{u}_h^{kn}$, we obtain the a posteriori estimate (4.20). □

The next estimate is derived by similar arguments.

Proposition 4.8. *The following a posteriori error estimate holds between the solutions $(\boldsymbol{u}^{kn}, p^{kn})_{1\le n\le N}$ to problem (3.1)–(3.3) and $(\boldsymbol{u}_h^{kn}, p_h^{kn})_{1\le n\le N}$ to problem (3.7)–(3.9),*

$$\sum_{m=1}^{n}\tau_m\left\|\frac{(\boldsymbol{u}^{km}-\boldsymbol{u}_h^{km})-(\boldsymbol{u}^{k,m-1}-\boldsymbol{u}_h^{k,m-1})}{\tau_m} + \boldsymbol{grad}_k(p^{km}-p_h^{km})\right\|^2_{L^2_1(\Omega)^3}$$

$$\lesssim \alpha\left\|\boldsymbol{u}_0^k - \Pi_{0h}\boldsymbol{u}_0^k\right\|^2_{L^2_1(\Omega)^3} + \sum_{m=1}^{n}\tau_m\Big((J_{km})^2 + (G_{km})^2 + \sum_{T\in\mathcal{T}_{kmh}}((\eta_T^{km})^2 + (\eta_{\partial T}^{km})^2)\Big).$$

4.3.1. Error of the three-dimensional solution

Using the same notation as above to introduce the truncated discrete solution

$$\breve{\boldsymbol{u}}^n_{\mathcal{K},h}(r,\theta,z) = \frac{1}{\sqrt{2\pi}}\sum_{|k|\le\mathcal{K}}\boldsymbol{u}_h^{kn}(r,z)e^{ik\theta} \quad\text{and}\quad \breve{p}^n_{\mathcal{K},h}(r,\theta,z) = \frac{1}{\sqrt{2\pi}}\sum_{|k|\le\mathcal{K}}p_h^{kn}(r,z)e^{ik\theta},$$

Theorem 4.9. *For n, $1\le n\le N$, we have the following a posteriori error estimate between $(\breve{\boldsymbol{u}}^n_{\mathcal{K}}, \breve{p}^n_{\mathcal{K}})$ defined in (3.4) and $(\breve{\boldsymbol{u}}^n_{\mathcal{K},h}, \breve{p}^n_{\mathcal{K},h})$*

$$\left\|\breve{\boldsymbol{u}}^n_{\mathcal{K}} - \breve{\boldsymbol{u}}^n_{\mathcal{K},h}\right\|^2_{L^2(\breve{\Omega})^3} \le \sum_{|k|\le\mathcal{K}}\Big(\left\|\boldsymbol{u}_0^k - \Pi_{0h}\boldsymbol{u}_0^k\right\|^2_{L^2_1(\Omega)^3} + c\Big(\left\|p_b^{kn} - i_{nh}p_b^{kn}\right\|^2_{H^{\frac{1}{2}}_{(k)}(\Gamma_p)}$$

$$+ \sum_{T\in\mathcal{T}_{knh}}(\eta_{\partial T}^{kn})^2\Big) + \frac{2}{\alpha}\sum_{m=1}^{n}\tau_m\Big(\left\|\boldsymbol{f}^{km} - \Pi_{nh}\boldsymbol{f}^{km}\right\|^2_{L^2_1(\Omega)^3} + \sum_{T\in\mathcal{T}_{kmh}}(\eta_T^{km})^2\Big)\Big),$$

and

$$\left\|\frac{(\breve{\boldsymbol{u}}^m_{\mathcal{K}} - \breve{\boldsymbol{u}}^m_{\mathcal{K},h}) - (\breve{\boldsymbol{u}}^m_{\mathcal{K}} - \breve{\boldsymbol{u}}^m_{\mathcal{K},h})}{\tau_m} + \boldsymbol{grad}(\breve{p}^m_{\mathcal{K}} - \breve{p}^m_{\mathcal{K},h})\right\|^2_{L^2(\breve{\Omega})^3}$$

$$\le \sum_{|k|\le\mathcal{K}}\Big(\alpha\left\|\boldsymbol{u}_0^k - \Pi_{0h}\boldsymbol{u}_0^k\right\|^2_{L^2_1(\Omega)^3} + \sum_{m=1}^{n}\tau_m\Big((J_{km})^2 + (G_{km})^2 + \sum_{T\in\mathcal{T}_{kmh}}((\eta_T^{km})^2 + (\eta_{\partial T}^{km})^2)\Big)\Big).$$

Proof. From Propositions 4.7 and 4.8 and the fact that

$$\left\|\breve{\boldsymbol{u}}^n_{\mathcal{K}} - \breve{\boldsymbol{u}}^n_{\mathcal{K},h}\right\|^2_{L^2(\breve{\Omega})^3} \le \sum_{|k|\le\mathcal{K}}\left\|\boldsymbol{u}^{kn} - \boldsymbol{u}_h^{kn}\right\|^2_{H^0_{(k)}(\Omega)^3},$$

and that

$$\left\| \frac{(\breve{\boldsymbol{u}}^m_{\mathcal{K}} - \breve{\boldsymbol{u}}^m_{\mathcal{K},h}) - (\breve{\boldsymbol{u}}^m_{\mathcal{K}} - \breve{\boldsymbol{u}}^m_{\mathcal{K},h})}{\tau_m} + \mathbf{grad}(\breve{p}^m_{\mathcal{K}} - \breve{p}^m_{\mathcal{K},h}) \right\|^2_{L^2(\breve{\Omega})^3}$$
$$\leq \sum_{|k|\leq\mathcal{K}} \left\| \frac{(\boldsymbol{u}^{km} - \boldsymbol{u}^{km}_h) - (\boldsymbol{u}^{k,m-1} - \boldsymbol{u}^{k,m-1}_h)}{\tau_m} + \mathbf{grad}_k(p^{km} - p^{km}_h) \right\|^2_{H^0_{(k)}(\Omega)^3}$$

we obtain the result. □

4.4. The efficiency of the indicators

We will prove an upper bound for the error indicators. For each $T \in \mathcal{T}_{knh}$, let ω_T denote the union of all triangles in $\mathcal{T}_{knh}$ that share at least an edge with T.

Proposition 4.10. *For each n, $1 \leq n \leq N$ and $T \in \mathcal{T}_{knh}$,*

$$\eta^{kn}_T \leq \alpha \left\| \boldsymbol{u}^{kn} - \boldsymbol{u}^{kn}_h \right\|_{L^2_1(T)^3} + \left\| \frac{(\boldsymbol{u}^{kn} - \boldsymbol{u}^{kn}_h) - (\boldsymbol{u}^{k,n-1} - \boldsymbol{u}^{k,n-1}_h)}{\tau_n} + \boldsymbol{grad}_k(p^{kn} - p^{kn}_h) \right\|_{L^2_1(T)^3} + \left\| \boldsymbol{f}^{kn} - \Pi_{nh}\boldsymbol{f}^{kn} \right\|_{L^2_1(T)^3}. \tag{4.23}$$

Proof. Using the fact that $p^{kn}_* - p^{kn}_{*h} = p^{kn} - p^{kn}_h - \mathcal{L}(p^{kn}_b - i_{nh}p^{kn}_b)$, and taking $\boldsymbol{v} = (\boldsymbol{u}^{k,n-1}_h - \Pi_{nh}\boldsymbol{u}^{k,n-1}_h)\chi_T$ in the first equation of (4.19), where χ_T is the characteristic function of T, we obtain

$$\left\| \boldsymbol{u}^{k,n-1}_h - \Pi_{nh}\boldsymbol{u}^{k,n-1}_h \right\|^2_{L^2_1(T)^3} = \alpha\tau_n \left(\boldsymbol{u}^{kn} - \boldsymbol{u}^{kn}_h, \overline{\boldsymbol{u}^{n-1}_h - \Pi_{nh}\boldsymbol{u}^{k,n-1}_h} \right)_{1,T}$$
$$+ \tau_n \left(\frac{(\boldsymbol{u}^{kn} - \boldsymbol{u}^{kn}_h) - (\boldsymbol{u}^{k,n-1} - \boldsymbol{u}^{k,n-1}_h)}{\tau_n} + \mathbf{grad}_k(p^{kn} - p^{kn}_h), \overline{\boldsymbol{u}^{k,n-1}_h - \Pi_{nh}\boldsymbol{u}^{k,n-1}_h} \right)_{1,T}$$
$$- \tau_n \int_T (\boldsymbol{f}^{kn} - \Pi_{nh}\boldsymbol{f}^{kn}) \cdot (\overline{\boldsymbol{u}^{k,n-1}_h - \Pi_{nh}\boldsymbol{u}^{k,n-1}_h}) r dr dz.$$

The Cauchy–Schwarz inequality yields

$$\left\| \boldsymbol{u}^{k,n-1}_h - \Pi_{nh}\boldsymbol{u}^{k,n-1}_h \right\|_{L^2_1(T)^3} \leq \alpha\tau_n \left\| \boldsymbol{u}^{kn} - \boldsymbol{u}^{kn}_h \right\|_{L^2_1(T)^3} + \tau_n \left\| \boldsymbol{f}^{kn} - \Pi_{nh}\boldsymbol{f}^{kn} \right\|_{L^2_1(T)^3}$$
$$+ \tau_n \left\| \frac{(\boldsymbol{u}^{kn} - \boldsymbol{u}^{kn}_h) - (\boldsymbol{u}^{k,n-1} - \boldsymbol{u}^{k,n-1}_h)}{\tau_n} + \mathbf{grad}_k(p^{kn} - p^{kn}_h) \right\|_{L^2_1(T)^3}.$$

Finally by multiplying this inequality by $\frac{1}{\tau_n}$ and from the expression of the a posteriori indicator η^{kn}_T, we obtain the desired estimate. □

Proposition 4.11. *For each n, $1 \leq n \leq N$ and $T \in \mathcal{T}_{knh}$,*

$$\eta^{kn}_{\partial T} \leq c \left\| \boldsymbol{u}^{kn} - \boldsymbol{u}^{kn}_h \right\|_{L^2_1(\omega_T)^3}. \tag{4.24}$$

Proof. By means of a fixed lifting operator on the reference element $\widehat{T}$ and by using the affine transformation that maps $\widehat{T}$ onto T, we construct for each $e \in \mathcal{E}_T$ a lifting operator $\mathcal{L}_{e,T}$ such that for each polynomial φ on e vanishing on ∂e, $\mathcal{L}_{e,T}\varphi$ is a polynomial on T vanishing on $\partial T \setminus e$ and equal to φ on e.

Let b_e be the bubble function on e, i.e., the product of the barycentric coordinates associated with the vertices of e. For each $e \in \mathcal{E}^0_T$, we denote by T' the other element of $\mathcal{T}_{knh}$ that contains e. In the second equation of (4.19), we take $q^n_h = 0$ and $q = q^{kn}_e$, with

$$q^{kn}_e = \begin{cases} \mathcal{L}_{e,T}([\boldsymbol{u}^{kn}_h \cdot \boldsymbol{n}_e]_e b_e) & \text{on } T, \\ \mathcal{L}_{e,T'}([\boldsymbol{u}^{kn}_h \cdot \boldsymbol{n}_e]_e b_e) & \text{on } T', \\ 0 & \text{elsewhere.} \end{cases}$$

Then, we obtain

$$\overline{b_1^k}\left(\boldsymbol{u}^{kn}-\boldsymbol{u}_h^{kn}, q_e^{kn}\right)=\langle g^{kn}, q_e^{kn}\rangle_{\Gamma_u}-\frac{1}{2}\sum_{T\in\mathcal{T}_{knh}}\left(\sum_{e\in\mathcal{E}_{nh}^{\Gamma_u}}\int_e[\boldsymbol{u}_h^{kn}\cdot\boldsymbol{n}_e]_e(\tau)\overline{q_e^{kn}}(\tau)d\tau\right).$$

On the other hand,

$$q_e^{kn}(\tau)=\mathcal{L}_{e,T}([\boldsymbol{u}_h^{kn}\cdot\boldsymbol{n}_e]_e b_e)\chi_T+\mathcal{L}_{e,T'}([\boldsymbol{u}_h^{kn}\cdot\boldsymbol{n}_e]_e b_e)\chi_{T'}=2[\boldsymbol{u}_h^{kn}\cdot\boldsymbol{n}_e]_e b_e.$$

Then

$$\left\|[\boldsymbol{u}_h^{kn}\cdot\boldsymbol{n}_e]_e b_e^{\frac{1}{2}}\right\|_{L_1^2(e)}^2\leq\left\|\boldsymbol{u}_h^{kn}-\boldsymbol{u}^{kn}\right\|_{L_1^2(T\cup T')^3}\left|q_e^{kn}\right|_{H_{(k)}^1(T\cup T')}. \tag{4.25}$$

Recall the following inverse inequality, for each constant λ, see [10, Lem. 3.3],

$$\|\lambda\|_{L_1^2(e)}\leq c\left\|\lambda b_e^{\frac{1}{2}}\right\|_{L_1^2(e)}\quad\text{and}\quad\left|\mathcal{L}_{e,T}(\lambda b_e)\right|_{H_{(k)}^1(T)}\leq c h_e^{-\frac{1}{2}}\|\lambda\|_{L_1^2(e)}.$$

The expression of $\eta_{\partial T}^{kn}$ and the first inverse inequality, yield

$$\eta_{\partial T}^{kn}\leq c\Big(\sum_{e\in\mathcal{E}_{nh}^{\Gamma_u}}h_e^{\frac{1}{2}}\left\|[\boldsymbol{u}_h^{kn}\cdot\boldsymbol{n}_e]_e b_e^{\frac{1}{2}}\right\|_{L_1^2(e)}\Big).$$

Using estimate (4.25) we obtain

$$\eta_{\partial T}^{kn}\leq c\Big(\sum_{e\in\mathcal{E}_{nh}^{\Gamma_u}}h_e^{\frac{1}{2}}\left\|\boldsymbol{u}_h^{kn}-\boldsymbol{u}^{kn}\right\|_{L_1^2(T\cup T')^3}^{\frac{1}{2}}\left|\mathcal{L}_{e,T}([\boldsymbol{u}_h^{kn}\cdot\boldsymbol{n}_e]_e b_e)\right|_{H_{(k)}^1(T\cup T')}^{\frac{1}{2}}\Big).$$

By inserting the second inverse inequality into this last inequality we obtain the bound on the second indicator $\eta_{\partial T}^{kn}$. □

To establish a global error, we assemble all the estimations obtained in sections above. To do so, we first define the following time and spacial error

$$\begin{aligned}\varepsilon_\tau=&\sup_{1\leq m\leq n}\left\|\boldsymbol{u}^k(\cdot,t_m)-\boldsymbol{u}^{km}\right\|_{L_1^2(\Omega)^3}+\left\|\partial_t(\boldsymbol{u}^k-\boldsymbol{u}_\tau^k)\right\|_{L^2(0,t_n;L_1^2(\Omega)^3)}\\&+\left\|p^k-p_\tau^k\right\|_{L^2(0,t_n;H_{(k)}^1(\Omega))},\\\varepsilon_h=&\sup_{1\leq m\leq n}\left\|\boldsymbol{u}^{km}-\boldsymbol{u}_h^{km}\right\|_{L_1^2(\Omega)^3}\\&+\sum_{m=1}^n\tau_m\left\|\frac{(\boldsymbol{u}^{km}-\boldsymbol{u}_h^{km})-(\boldsymbol{u}^{k,m-1}-\boldsymbol{u}_h^{k,m-1})}{\tau_m}+\mathbf{grad}_k(p^{km}-p_h^{km})\right\|_{L_1^2(\Omega)^3}^2.\end{aligned}$$

Next, by combining all the a posteriori results, we observe that, up to the terms involving the data, the full error $\varepsilon_\tau+\varepsilon_h$ is equivalent to the sum

$$\Big(\sum_{m=1}^n(\eta_m^k)^2+\tau_m\sum_{T\in\mathcal{T}_{kmh}}(\eta_T^{km}+\eta_{\partial T}^{km})^2\Big)^{\frac{1}{2}},$$

with equivalence constants independent of τ and h_n. Moreover, estimate (4.14) is local in time and estimates (4.23) and (4.24) are local with respect to both the time and space variables. Therefore these estimates are fully optimal. Hence, a simple adaptivity strategy relying on these indicators can be applied for adapting both the time step and the mesh.

5. Adaptivity strategy

As standard, the adaptivity strategy that we use combines three steps, an initialization step, an adaptation step in time and an adaptation step in space. We fix a positive tolerance η^*.

Step 1: Initialization We fix a triangulation $\mathcal{T}_{0h}$ of Ω such that the quantities which appear in Propositions 4.7 and 4.8, namely:

$$\left\|\boldsymbol{u}_0^k-\Pi_{0h}\boldsymbol{u}_0^k\right\|_{L_1^2(\Omega)^3},\ \left\|\boldsymbol{f}^{kn}-\Pi_{nh}\boldsymbol{f}^{kn}\right\|_{L_1^2(\Omega)^3}\ \text{and}\ \left\|p_b^{kn}-i_{nh}p_b^{kn}\right\|_{H_{(k)}^{\frac{1}{2}}(\Gamma_p)}$$

are smaller than η^*. This condition is possible for smooth data thanks to the approximation properties of the finite element spaces involved in the discretization.

Step 2: Time adaptivity Assuming that the time step τ_n, the triangulation $\mathcal{T}_{n-1,h}$ and the discrete solution $(\boldsymbol{u}_h^{k,n-1}, p_h^{k,n-1})$ are known. We first initialize $\mathcal{T}_{nh}$ equal to $\mathcal{T}_{n-1,h}$. Next, we compute the first solution $(\boldsymbol{u}_h^{kn}, p_h^{kn})$ to problem (3.7)–(3.9) and the corresponding error indicators η_n^k defined in (4.1). Finally,

- if η_n^k is smaller than η^*, we proceed to the spatial adaptivity step;
- else, we divide τ_n by two (or by a constant times η_n^k/η^*) and perform a new computation.

Of course, this step can be iterated a number of times. This leads to the final value of τ_n.

Step 3: Spatial adaptivity

Assuming that the time step τ_n and the triangulation $\mathcal{T}_{nh}$ are known. We compute the discrete solution $(\boldsymbol{u}_h^{kn}, p_h^{kn})$ to problem (3.7)–(3.9) corresponding to this triangulation. We then calculate the error indicators η_T^{kn} and $\eta_{\partial T}^{kn}$ defined in (4.18) and their mean values $\bar{\eta}_T^{kn}$ and $\bar{\eta}_{\partial T}^{kn}$, respectively.

Concerning the adaptivity, we perform it in three substeps:

(i) All $e \in \mathcal{E}_{nh}^{\Gamma_u}$ (with obvious notation) such that $\eta_{\partial T}^{kn}$ are larger than $\max\{\eta^*, \bar{\eta}_{\partial T}^{kn}\}$ are divided into N equal segments, where N is proportional to the ratio $\eta_{\partial T}^{kn}/\max\{\eta^*, \bar{\eta}_{\partial T}^{kn}\}$. This gives rise to a new set $e \in \mathcal{E}_{n+1,h}^{\Gamma_u}$.

(ii) A new triangulation on Ω is constructed using these new edges.

(iii) The triangulation $\mathcal{T}_{nh}$ is refined and coarsened according to the following criterion: the diameter of a new element contained in T or containing T is proportional to h_T times the ratio $\bar{\eta}_T^{kn}/\eta_T^{kn}$. This gives rise to the new triangulation $\mathcal{T}_{n+1,h}$.

Of course, the adaptation step is iterated either a finite number of times or until the Hilbertian sum of all error indicators, namely

$$\Big(\sum_{m=1}^{n}(\eta_m^k)^2 + \tau_m \sum_{T\in\mathcal{T}_{kmh}} (\eta_T^{km} + \eta_{\partial T}^{km})^2\Big)^{\frac{1}{2}} \quad \text{become smaller than tolerance} \quad \eta^*.$$

Note that, this strategy is very similar to that in [18,19].

6. Numerical experiment

To show the effectiveness of our numerical scheme, we present in this section the following simulation that we have carried out using FreeFem++ [20]. The computational domain $\breve{\Omega}$ is generated by the L-shaped meridian domain Ω defined by

$$\Omega =]0, 1[\times]-2, 0[\cap]0, 2[\times]0, 2[.$$

We denote by Γ_0 the intersection between $\breve{\Omega}$ and axis $r = 0$, and the boundary $\Gamma = \partial\Omega \cup \Gamma_0$ is divided into two parts Γ_p and Γ_u such that: Γ_p coincides with the intersection of Γ and the plan $z = 0$.

We solve Darcy equations with data $\alpha = 0.1$, pressure $p_b = 0$ on Γ_p, g_u defined on Γ_u as:

$$g_u(r, 1) = \left(1 - r^2\right)\,\sin(t), \qquad g_u(0, z) = \left(1 - z^2\right)\,\sin(t),$$
$$g_u(r, 2) = \left(4 - r^2\right)\,t, \qquad g_u(2, z) = \left(4 - z^2\right)\,t$$

and the source term $\boldsymbol{f}$ is equal to $(1, 0)$. The discrete solution corresponds to $\mathcal{K} = 3$.

To build a reference solution $(\boldsymbol{u}_e, p_e)$ which will serve as the exact solution, we consider a uniform triangular fine mesh, where the size mesh h is taken equal to $h_{ref} = 0.000985038$ (the number of triangles = 225,452 and the number of vertices = 113,495) and a uniform small time step $\tau = \tau_{ref} = 10^{-3}$.

In the first test we use a uniform triangular grid with reference mesh size $h = h_{ref}$ and vary the time step from $\tau = 1/10$ to $\tau = 1/320$.

In the second test, all computations are performed using the reference time step $\tau = \tau_{ref}$ and the coarse mesh such that its size $h = 0.0891014$ was halved successively.

We introduce the following notation to describe the energy errors of velocity and pressure at final time $T = 1$:

$$E(\boldsymbol{u}) = \|\boldsymbol{u}_e(\cdot, 1) - \boldsymbol{u}_h^N\|, \qquad E(p) = \|p_e(\cdot, 1) - p_h^N\|,$$
$$E(\boldsymbol{u}, p) = \left(E(\boldsymbol{u})^2 + E(p)^2\right)^{1/2}, \qquad \eta^N = \sqrt{\tau}\,\left\|\boldsymbol{u}_h^N - \boldsymbol{u}_h^{N-1}\right\|.$$

We denote by $\mathcal{O}(\boldsymbol{u})$, $\mathcal{O}(p)$, $\mathcal{O}(\boldsymbol{u}, p)$ the rates of convergence of $\boldsymbol{u}$, p and $(\boldsymbol{u}, p)$ respectively. In Table 6.1, for the very small mesh size h (degree of freedom (DOF) = 791,387), we observe that the convergence rate $\mathcal{O}(\boldsymbol{u}, p)$ is approximatively equal to 1 and the indicator η^N decreases with respect to the time step τ which meets our analysis.

Table 6.2 shows that for a fixed time step $\tau = \tau_{ref}$, all errors decrease with respect to the size mesh h. However, the convergence rate is $\mathcal{O}(\boldsymbol{u}) < 1$ even on fine meshes. This could be due to the time discretization error, which in this case, pollutes the finite element approximation.

Finally, using the adaptivity strategy, we present in Table 6.3 the evolution of the total error $E(\boldsymbol{u}, p)$, the indicator η^N and the convergence order $\mathcal{O}(\boldsymbol{u}, p)$ with respect to the time step. For these computations, DOF does not change too much

Table 6.1
The energy errors, convergence orders and indicators for decreasing time steps in reference mesh.

Time step τ	DOF	$E(\boldsymbol{u}, p)$	Indicator η^N	Order $\mathcal{O}(\boldsymbol{u}, p)$
1/10	791,387	0.609038	0.0480949	–
1/20	791,387	0.304934	0.0164095	0.998
1/40	791,387	0.150187	0.00569467	1.021
1/80	791,387	0.0721612	0.0019943	1.057
1/160	791,387	0.0329877	0.000701707	1.129
1/320	791,387	0.0133611	0.000247491	1.3

Table 6.2
The energy errors, convergence orders and indicators for uniformly refined meshes.

Mesh size h	DOF	$E(\boldsymbol{u})$	E(p)	η^N	$\mathcal{O}(\boldsymbol{u}) - \mathcal{O}(p)$
0.0333496	871	0.486614	0.0693221	0.000483728	–
0.0181035	3,211	0.283261	0.0204435	0.000481757	0.78 – 1.76
0.00843482	12,630	0.18849	0.00914296	0.000481295	0.58 – 1.16
0.0039905	49,857	0.117566	0.00305163	0.000481062	0.68 – 1.58
0.00197026	197,006	0.072015	0.00103792	0.000480987	0.70 – 1.55

Table 6.3
The errors, convergence orders and indicators for decreasing time steps on the adaptive mesh.

τ	DOF	$E(\boldsymbol{u}, p)$	η^N	$\mathcal{O}(\boldsymbol{u}, p)$
1/10	154,192	0.612676	0.0480993	–
1/20	154,944	0.306787	0.0164091	0.9978
1/40	154,213	0.155407	0.00569445	0.981
1/80	153,878	0.08374	0.00199421	0.892
1/160	154,195	0.0540663	0.000701676	0.631
1/320	153,787	0.0462765	0.00024748	0.2244

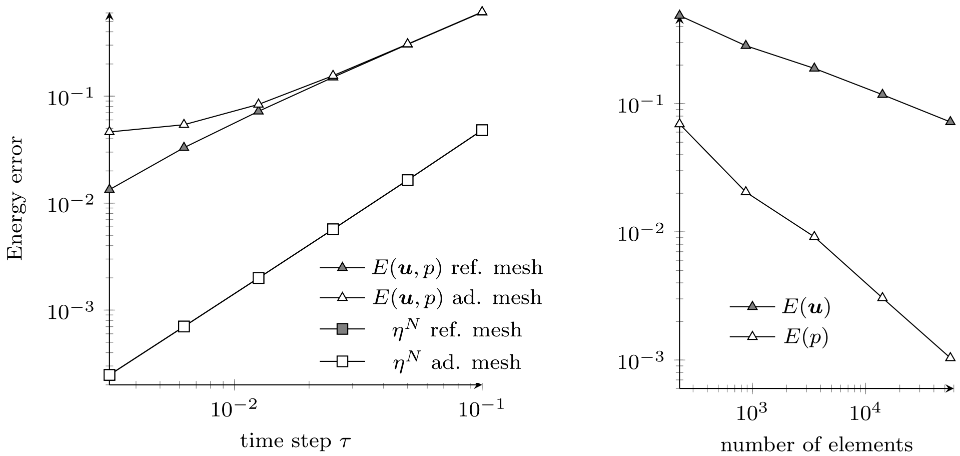

Fig. 6.1. On the right: Results by adaptivity strategy with respect to the degree of freedom DOF. On the left: Results by adaptivity strategy and a uniform refined meshes with respect to the time step.

$\approx$ 154,000. We observe that between $\tau = 1/10$ and $\tau = 1/80$, the obtained solutions are good and can be compared with those computed in the first test, see Table 6.1.

However, the CPU time is 5 times better when we use the adaptivity strategy. This is due especially to the size of the resulting systems, i.e.: DOF = 197,006 (adaptivity strategy) and DOF = 791,387 (reference mesh). Whereas for $\tau > 1/80$, errors and orders deteriorated, once again it is due to the error arising from the time discretization. Fig. 6.1 shows clearly these remarks. Fig. 6.2 presents the initial and final adapted meshes near the re-entrant corners and the corresponding velocity and pressure are plotted in Fig. 6.3.

7. Conclusion

The system of unsteady Darcy's equations in a three-dimensional axisymmetric domain considered here modeled the time-dependent flow of an incompressible fluid such as water in a rigid porous material. By writing the Fourier expansion

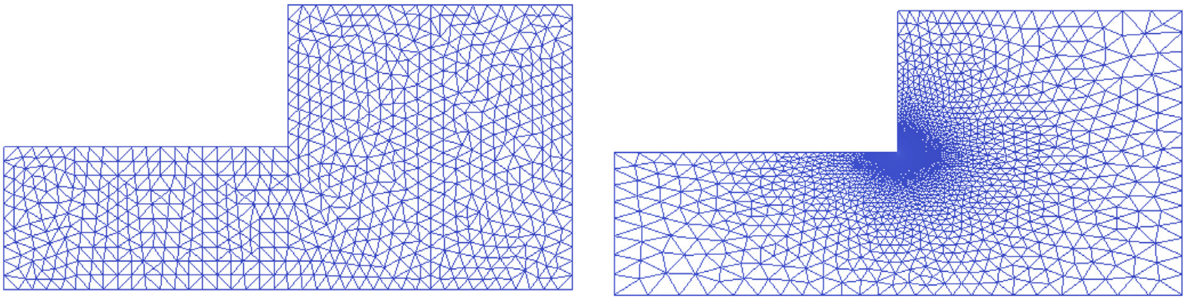

Fig. 6.2. Initial mesh on the left and the final mesh on the right.

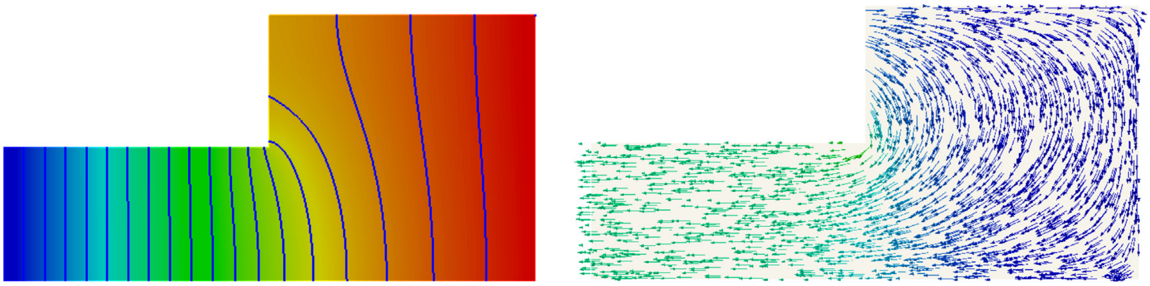

Fig. 6.3. On the left: The isobar of the pressure. On the right: The vector field of the velocity.

of its solution with respect to the angular variable, we have observed that each Fourier coefficient satisfies a system of equations on the meridian domain. We have proposed a discretization of these equations in the case of general solution. This discretization is based on the backward Euler's scheme for the time variable and the finite elements for the space variables. We have proved a posteriori error estimates that allow for an efficient adaptivity strategy both for the time steps and the meshes. We have applied this strategy to building a mesh refinement, which we have tested in the L-shaped meridian domain. Numerical tests confirm our theoretical findings and show their robustness by (for instance) reducing the CPU time.

In future work, we will use others a posteriori error estimators for the time-dependent Darcy system in an axisymmetric domain with mixed boundary conditions. The question that arises naturally, which approach is better than another one, in certain sense, to solve this problem. Our attention will be carried towards the following approaches: the flux-jump error estimators, see [21], and the patch-recovery method, see [22].

References

[1] K.R. Rajagobal, On a hierarchy of approximate models for flows of incompressible fluids through porous solids, Math. Models and Methods Appl. Sci. 17 (2007) 215–252.

[2] C. Bernardi, M. Dauge, Y. Maday, Spectral methods for axisymmetric domains, in: Series in Applied Mathematics, vol. 3, Gauthier-Villars, North-Holland, 1999, p. 3.

[3] C. Bernardi, A.Y. Orfi, Finite element discretization of the time dependent axisymmetric Darcy problem, J. Span. Soc. Appl. Math. SEMA (2015) 53–80.

[4] C. Bernardi, V. Girault, K. Rajagopal, Discretisation of an unsteady flow through a porous solid modeled by Darcy's equations, Math. Models Methods Appl. Sci. 18 (12) (2008) 2087–2123.

[5] A.Y. Orfi, D. Yakoubi, A priori error analysis of an Euler implicit, finite element approximation of the unsteady Darcy problem in an axisymmetric domain, Adv. Appl. Math. Mech. 10 (2) (2018) 301–321.

[6] K. Eriksson, C. Johnson, Adaptive finite element methods for parabolic problems. I. A linear model problems, SIAM J. Numer. Anal. 28 (1991) 43–77.

[7] K. Eriksson, C. Johnson, Adaptive finite element methods for parabolic problems. IV. Nonlinear problems, SIAM J. Numer. Anal. 32 (1995) 1729–1749.

[8] R. Verfürth, A posteriori error estimates techniques for non-linear elliptic and parabolic pdes, Rev. Européenne élém. Finis 9 (2000) 377–402.

[9] A. Bergam, C. Bernardi, Z. Mghazli, A posteriori analysis of the finite element discretization of some parabolic equations, Math. Comp. 74 (2005) 1117–1138.

[10] R. Verfürth, A Review of a Posteriori Error Estimation and Adaptive Mesh-Refinement Techniques, Wiley, Teubner, 1996.

[11] C. Bernardi, M. Dauge, Y. Maday, Polynomials in weighted Sobolev spaces: Basics and trace liftings, in: Internal Report, vol. 92039, Laboratoire d'Analyse Numérique, Université Pierre et Marie Curie, Paris, 1992.

[12] V. Girault, P.-A. Raviart, Finite element methods for Navier–Stokes equations, in: Theory and Algorithms, Springer-Verlag, Berlin, 1986.

[13] Y. Achdou, C. Bernardi, F. Coquel, A priori and a posteriori analysis of finite volume discretizations of Darcy's equations, Numer. Math. 96 (2003) 17–42.

[14] C. Johnson, Y.-Y. Nie, V. Thomée, An a posteriori error estimate and adaptive timestep control for a backward Euler discretization of a parabolic problem, SIAM J. Number. Anal. 27 (1990) 277–291.

[15] L.R. Scott, S. Zhang, Finite element interpolation of non-smooth functions satisfying boundary conditions, Math. Comp. 54 (1900) 483–493.

[16] C. Bernardi, Y. Maday, F. Rapetti, Discrétisations variationelles de problémes aux limites elliptiques, in: Collection Mathématiques et Applications, vol. 45, Springer-Verlag, 2004.

[17] Z. Belhachmi, C. Bernardi, S. Deparis, Weighted Clément operator and application to the finite element discretization of the axisymmetric Stokes problem, Numer. Math. 105 (2006) 217—247.
[18] C. Bernardi, L. El Alaoui, Z. Mghazli, A posteriori analysis of a space and time discretization of a nonlinear model for the flow in partially saturated porous media, IMA J. Numer. Anal. 34 (2014) 1002–1036.
[19] C. Bernardi, E. Suli, Time and space adaptivity for the second-order wave equation, Math. Models. Methods Appl. Sci. 15 (2005) 199–225.
[20] F. Hecht, New development in FreeFem++, J. Numer. Math. 20 (2012) 251–266.
[21] T. Grätsch, K.-J. Bathe, A posteriori error estimation techniques in practical finite element analysis, Comput. Struct. 83 (4–5) (2005) 235–265.
[22] O.C. Zienkiewicz, J.Z. Zhu, The superconvergent patch recovery and a posteriori error estimates II. Error estimates and adaptivity, Internat. J. Numer. Methods Engrg. 33 (7) (1992) 1365–1382.